Electronic Supplementary Information

Encapsulation and solid state sequestration of gases by calix[6]arene-based molecular containers

Roy Lavendomme,[a,b] Daniela Ajami,[a,b] Steven Moerkerke,[a] Johan Wouters,[c] Kari Rissanen,[d] Michel Luhmer,[b] Ivan Jabin[a]**

[a] Laboratoire de Chimie Organique, Université libre de Bruxelles (ULB), Avenue F.D. Roosevelt 50, CP160/06, B-1050 Brussels, Belgium. E-mail: ijabin@ulb.ac.be
[b] Laboratoire de Résonance Magnétique Nucléaire Haute Résolution, Université libre de Bruxelles (ULB), Avenue F.D. Roosevelt 50, CP160/08, B-1050 Brussels, Belgium. E-mail: mluhmer@ulb.ac.be
[c] Département de Chimie, Université de Namur (UNamur), Rue de Bruxelles 61, B5-5000 Namur, Belgium.
[d] University of Jyväskylä, Department of Chemistry, Nanoscience Center, P.O. Box 35, FI-40014, Finland.

Table of contents

Experimental Section

The starting calixarene **3** was synthesized according to the procedure described in the literature.[1] The reactions were not performed under inert atmosphere unless otherwise stated. Solvents were distilled prior to use. Anhydrous dichloromethane was obtained from distillation over CaH_2. Silica gel (230-400 mesh) was used for flash chromatography. High resolution mass spectra were recorded with either TOF or Q-TOF ESI+/- spectrometers. Melting points (mp) are uncorrected. ATR-FTIR spectra were recorded at room temperature. NMR spectra were recorded either at 7.0, 9.4 or 14.1 Tesla. NMR analyses requiring more than 3 bar of gas pressure were performed in a 5 mm Wilmad 507-PV-7 valve tube; gases were pressurized up to about 12 bars on a pressure/vacuum line. Traces of residual solvents were used as internal standards for ^{1}H (7.26 ppm for $CHCl_3$, 5.32 ppm for $CHDCl_2$, 6.00 ppm for $CDCl_2CHCl_2$) and ^{13}C (77.16 ppm for $CDCl_3$, 73.78 ppm for $(CDCl_2)_2$) chemical shift referencing. $CFCl_3$ (0.00 ppm) was used as internal standard for ^{19}F chemical shift referencing. Abbreviations: s: singlet, d: doublet, br: broad signal, m: massif. Bac stands for *tert*-Butylaminocarbonyl. Imi stands for imidazolidin-2-one. “in” and “out” stand for inside and outside the cavity of the molecular container.

[1] R. Lavendomme, A. Leroy, M. Luhmer and I. Jabin, *J. Org. Chem.*, 2014, **79**, 6563.

Synthesis of *p*-*t*Bu-calix[6]arene-penta-Bac-mono-Boc **4**

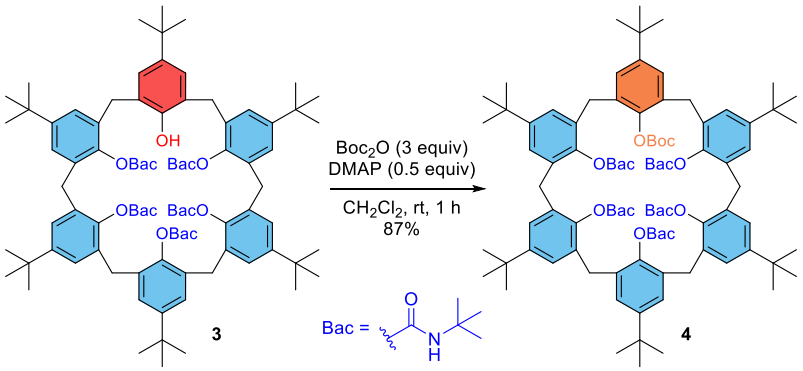

N,*N*-dimethylaminopyridine (6 mg, 0.05 mmol) and Boc_2O (69 µL, 66 mg, 0.30 mmol) were added to a solution of calixarene **3** (147 mg, 0.100 mmol) in CH_2Cl_2 (5 mL). The mixture was stirred for 1 h at room temperature. The mixture was then concentrated under vacuum. The resulting solid was solubilized in CH_2Cl_2/CH_3CN (5:1, v/v) followed by crystallization through slow evaporation of the solvent under air. The remaining 1-2 mL of solvent was removed and the crystals were washed with CH_3CN (2×1 mL). The crystals were then dried under vacuum affording calixarene **4** as a white solid (136 mg, 0.0867 mmol). Yield: 87%.

R_f (CH_2Cl_2) = 0.28. Mp = 246°C (decomp.). IR (ATR) ν (cm^{-1}) = 2964, 1750, 1454, 1170. The ^1H and ^{13}C NMR spectra could not be completely assigned due to the presence of multiple conformers in slow exchange on the chemical shift time scale (*vide infra*). HRMS (ESI+): calcd for $C_{96}H_{141}N_6O_{13}$ $[M+NH_4]^+$ 1586.0551, found 1586.0552.

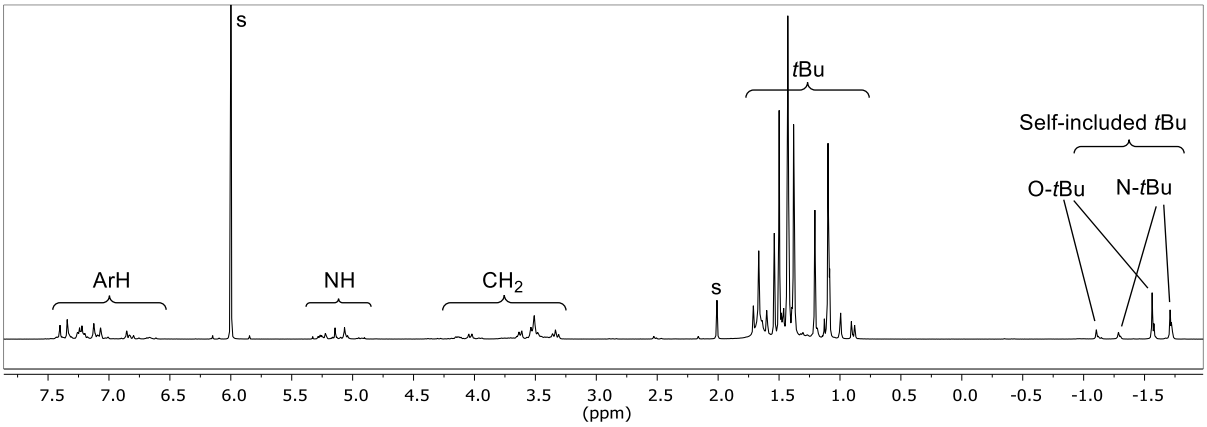

^1H NMR spectrum of **4** (600 MHz, $(CDCl_2)_2$, 298 K). s: residual solvents. This complex spectrum results from the overlapping signatures of multiple conformers in slow exchange rate on the chemical shift time scale, as shown by EXSY correlations observed in 2D ROESY spectra. Partial assignment was achieved through dqfCOSY, HSQC, HMBC and ROESY analyses (*vide infra*).

Synthesis of *p*-*t*Bu-calix[6]arene-mono-acetyl-penta-Bac **5**

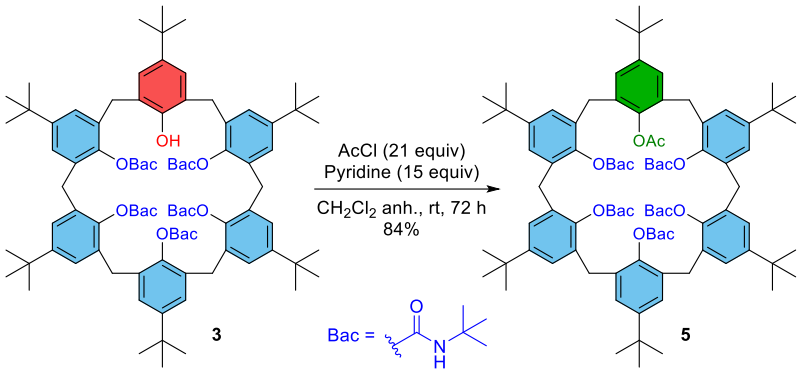

Pyridine (84 µL, 82 mg, 1.0 mmol) and acetyl chloride (100 µL, 111 mg, 1.41 mmol) were added to a solution of calixarene **3** (101 mg, 0.0687 mmol) in anhydrous CH_2Cl_2 (10 mL) under inert atmosphere. The mixture was stirred for 72 h at room temperature. The mixture was then extracted with water and the organic layer was concentrated under vacuum. The resulting residue was purified by flash chromatography (CH_2Cl_2) affording calixarene **5** as a white solid (87 mg, 0.058 mmol). Yield: 84%.

R_f (CH_2Cl_2) = 0.23. Mp = 283°C (decomp.). IR (ATR) ν (cm^{-1}) = 2963, 1749, 1455, 1170. The ^1H and ^{13}C NMR spectra could not be completely assigned due to the presence of multiple conformers in slow exchange on the chemical shift time scale (*vide infra*). HRMS (ESI+): calcd for $C_{93}H_{131}N_5O_{12}Na$ $[M+Na]^+$ 1532.9686, found 1532.9689.

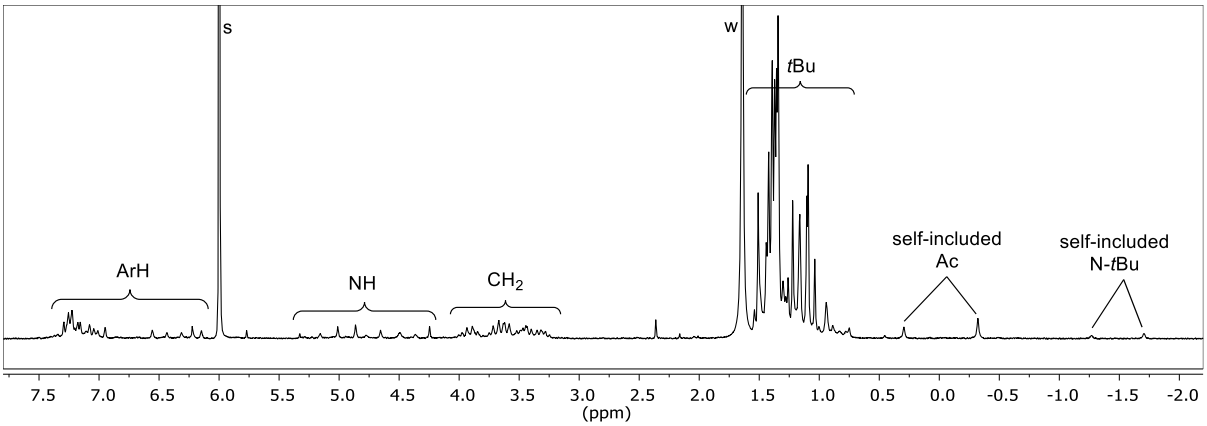

^1H NMR spectrum of **5** (400 MHz, $(CDCl_2)_2$, 298 K). s: residual solvent, w: residual water. This complex spectrum results from the overlapping signatures of multiple conformers in slow exchange rate on the chemical shift time scale, as shown by EXSY correlations observed in 2D ROESY spectra. Partial assignment was achieved through dqfCOSY, HSQC, HMBC and ROESY analyses (*vide infra*).

Crystallogenesis

The following two crystallogenesis methods were used to obtain crystals of gas inclusion complexes with molecular containers **1** and **4**:

Method A: Evaporation from a solution of molecular container in $(CHCl_2)_2$ under a flow of gas.

Method B: Cooling to 253 K a saturated solution of molecular container in $(CHCl_2)_2$ under about 2 bar of gas and letting it rest for 1 night or up to few days.

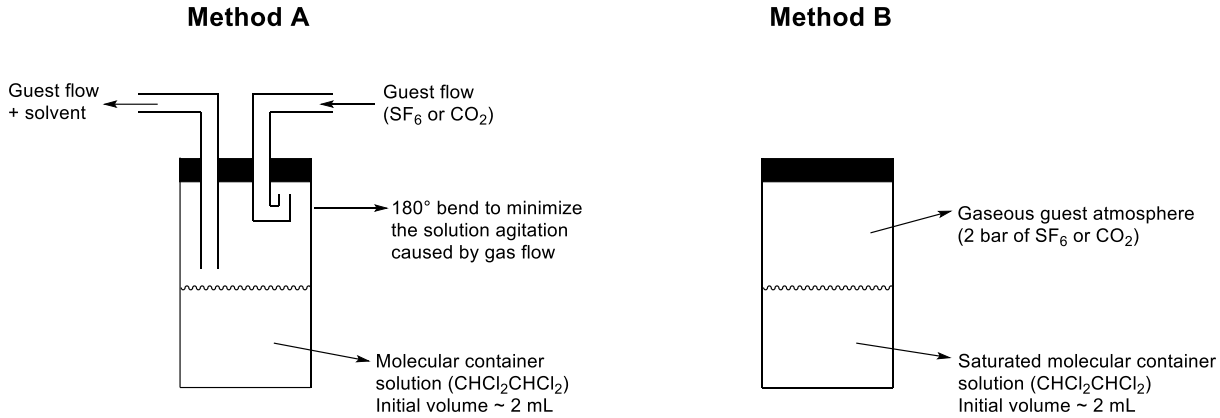

Figure S1. Schematic representation of the samples/devices used for crystallogenesis methods A and B.

Characterization of the new compounds by NMR spectroscopy

p-*t*Bu-calix[6]arene-penta-Bac-mono-Boc **4**

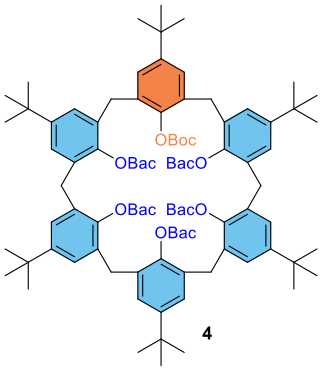

4

Among usual organic solvents, highest solubilities for molecular container **4** (*i.e.* several cg/mL) were observed in dichloromethane and 1,1,2,2-tetrachloroethane. For comparison, solubilities of *ca.* 4 and 80 mg/mL were observed in $(CHCl_2)_2$ for **1** and **4**, respectively. ^{1}H NMR spectra recorded at 298 K in CD_2Cl_2 and $(CDCl_2)_2$ show a high number of overlapping peaks of variable relative intensities due to the coexistence of multiple conformers in slow exchange on the chemical shift time scale (Figure S2). The spectrum recorded in $(CDCl_2)_2$ (*i.e.* a solvent too big to fit inside this molecular container cavity) shows mainly conformers of **4** self-including one Boc or Bac group (see HMBC, Figure S8). In contrast, the spectrum recorded in CD_2Cl_2 shows mainly conformers of **4** with no self-inclusion due to the encapsulation of a solvent molecule. ^{1}H spectra recorded in at higher temperature $(CDCl_2)_2$, up to 403 K, show significant signal broadening but fast conformational exchange could not be reached (Figure S3). The 2D-ROESY spectrum recorded at 298 K in this solvent shows numerous EXSY-type correlations confirming chemical exchange between several conformers of a single species (Figure S6).

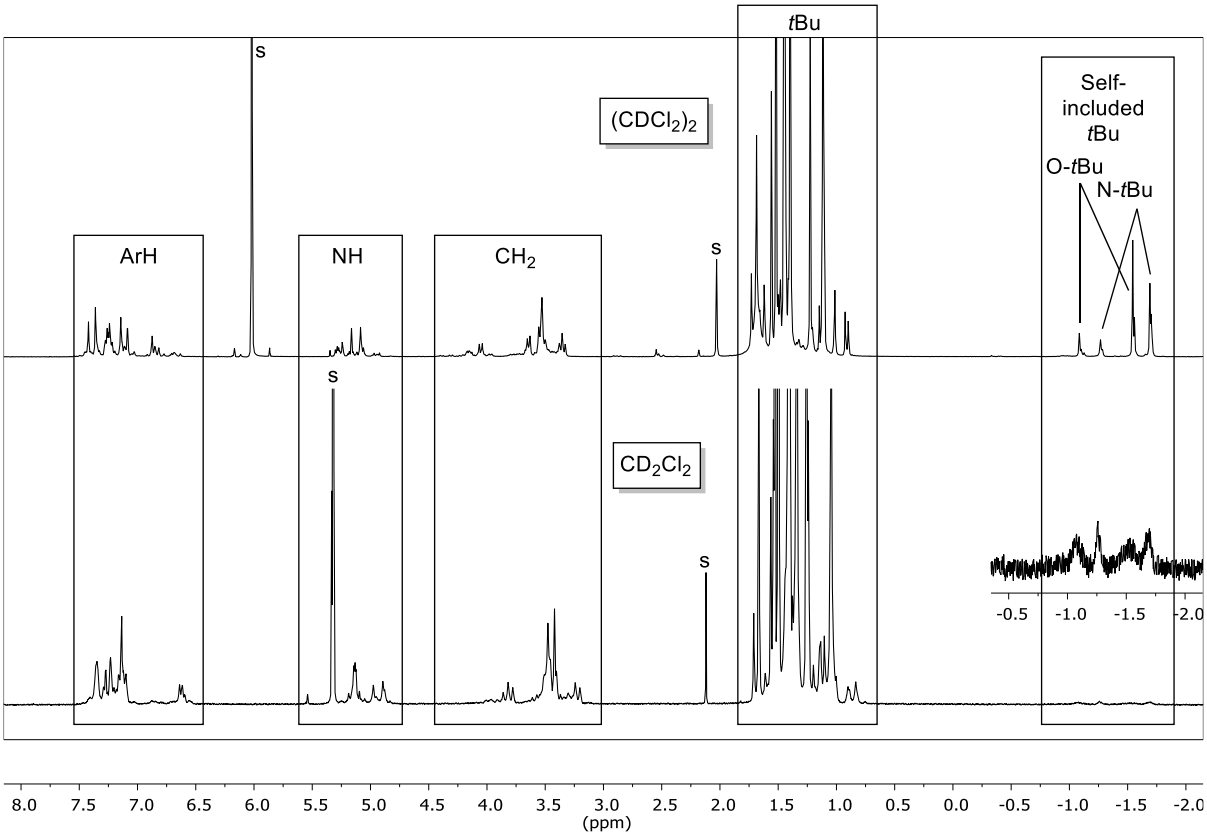

Figure S2. ^{1}H NMR spectra of **4** (Top: 600 MHz, $(CDCl_2)_2$, 298 K; Bottom: 400 MHz, CD_2Cl_2, 298 K). s: residual solvents.

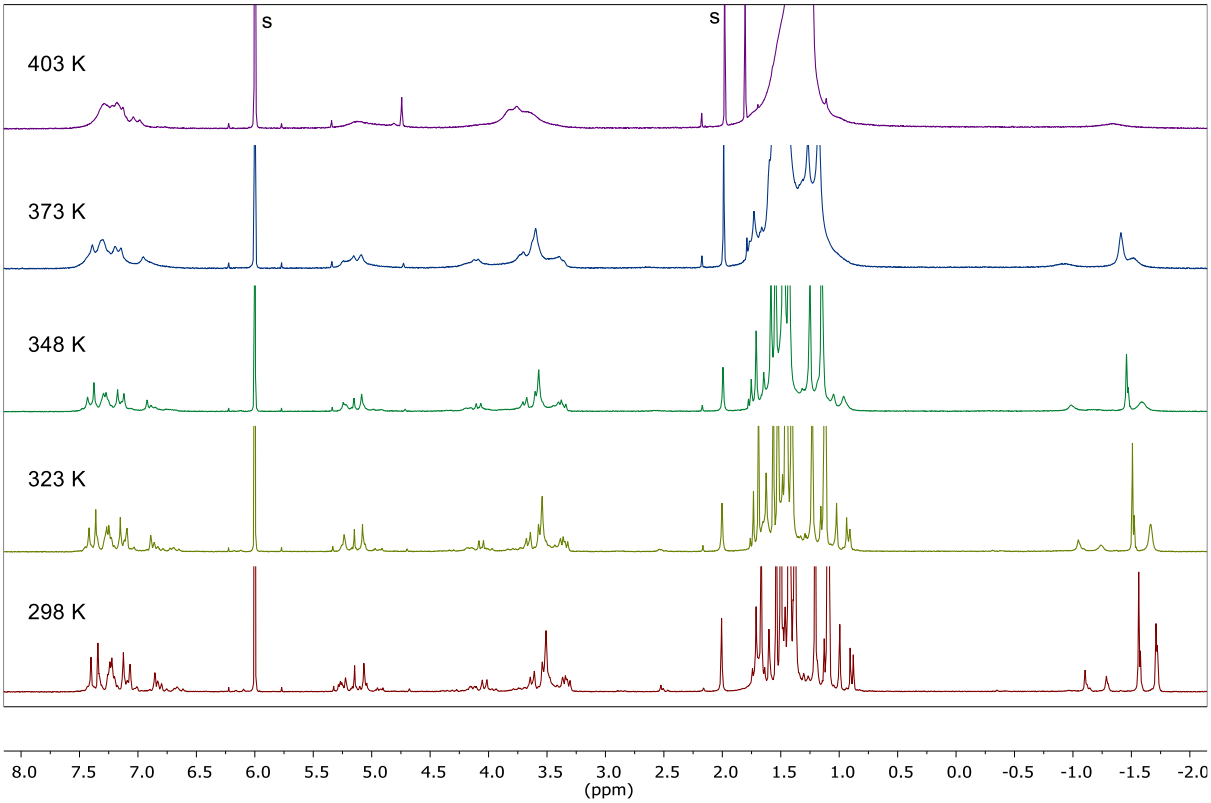

Figure S3. VT ^{1}H NMR spectra of **4** (400 MHz, $(CDCl_2)_2$). s: residual solvents.

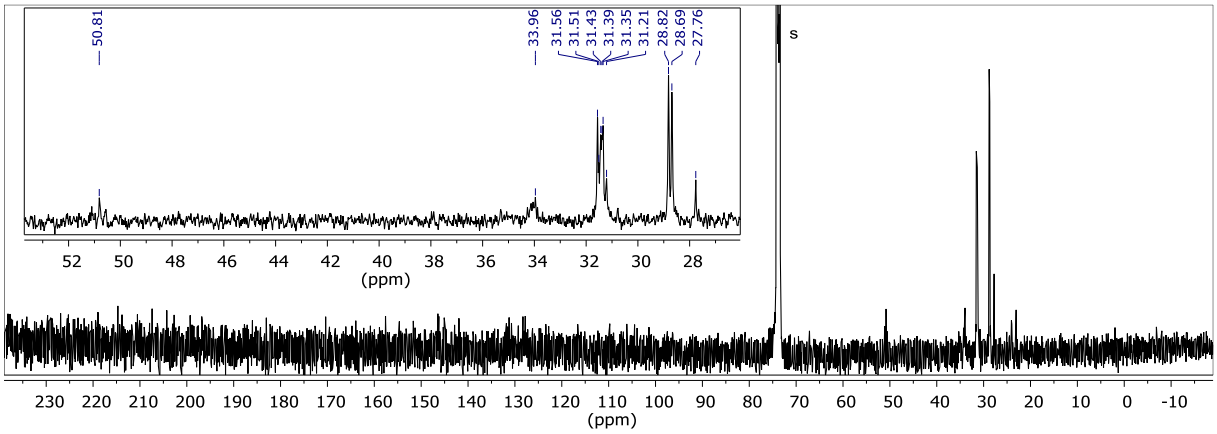

Figure S4. ^{13}C NMR spectra of **4** (100 MHz, $(CDCl_2)_2$, 298 K). s: residual solvent. Only few peaks are observed despite extensive signal averaging (*i.e.* 17500 scans) due to the presence of multiple conformers in slow exchange on the NMR chemical shift time scale. The following partial assignment relies on HSQC and HMBC spectra: N-**C** (~50 ppm), Ar-**C**H_2-Ar (~28-36 ppm), Ar-**C**-CH_3 (~34 ppm), Ar-C-**C**H_3 (~31 ppm), N-C-**C**H_3 (~28 ppm). These data are in agreement with the ^{13}C chemical shifts reported for similar compounds.[1,2,3]

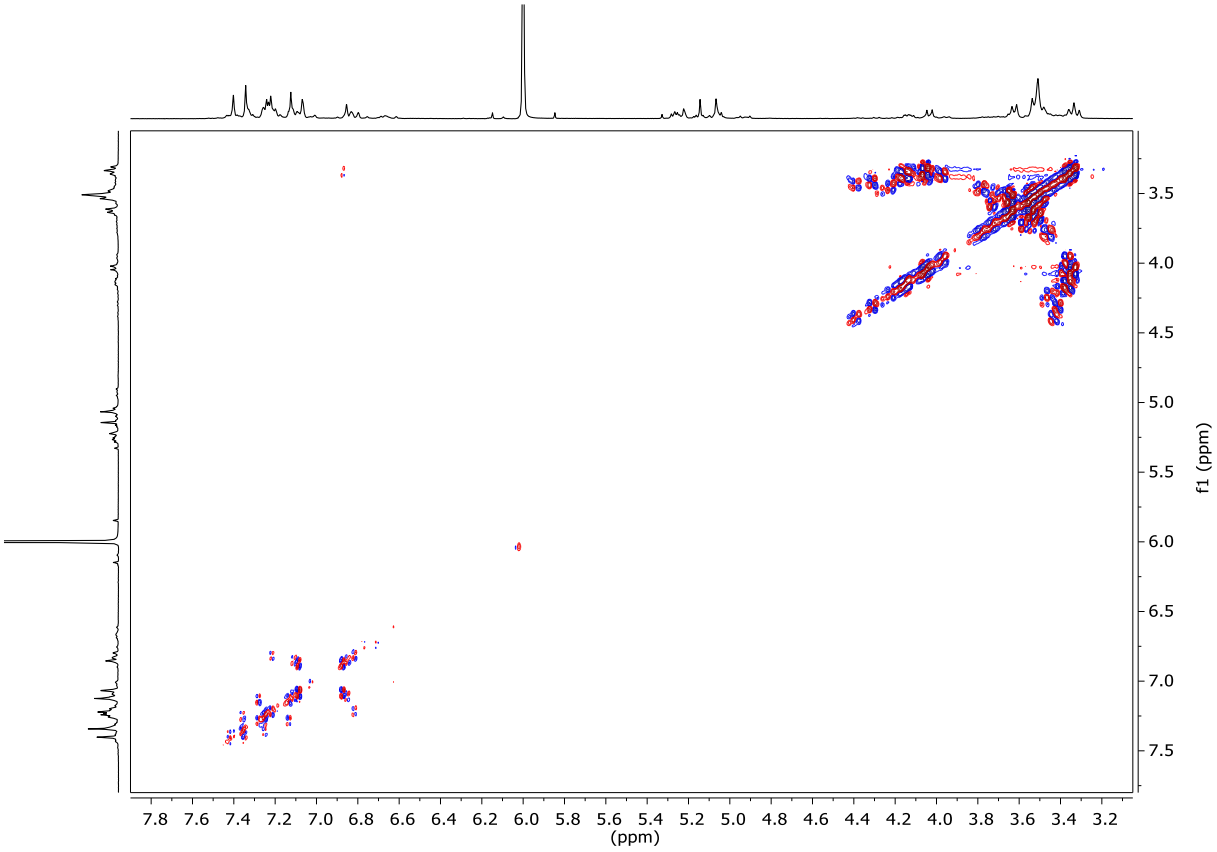

Figure S5: dqfCOSY spectrum of **4** (600 MHz, $(CDCl_2)_2$, 298 K).

[2] R. Lavendomme, P. J. Cragg, P. M. Marcos, M. Luhmer and I. Jabin, *Org. Lett.*, 2015, **17**, 5690.

[3] R. Lavendomme, V. Malytskyi, J. Vandermeersch, M. Luhmer and I. Jabin, *Synthesis*, 2017, **49**, 1009.

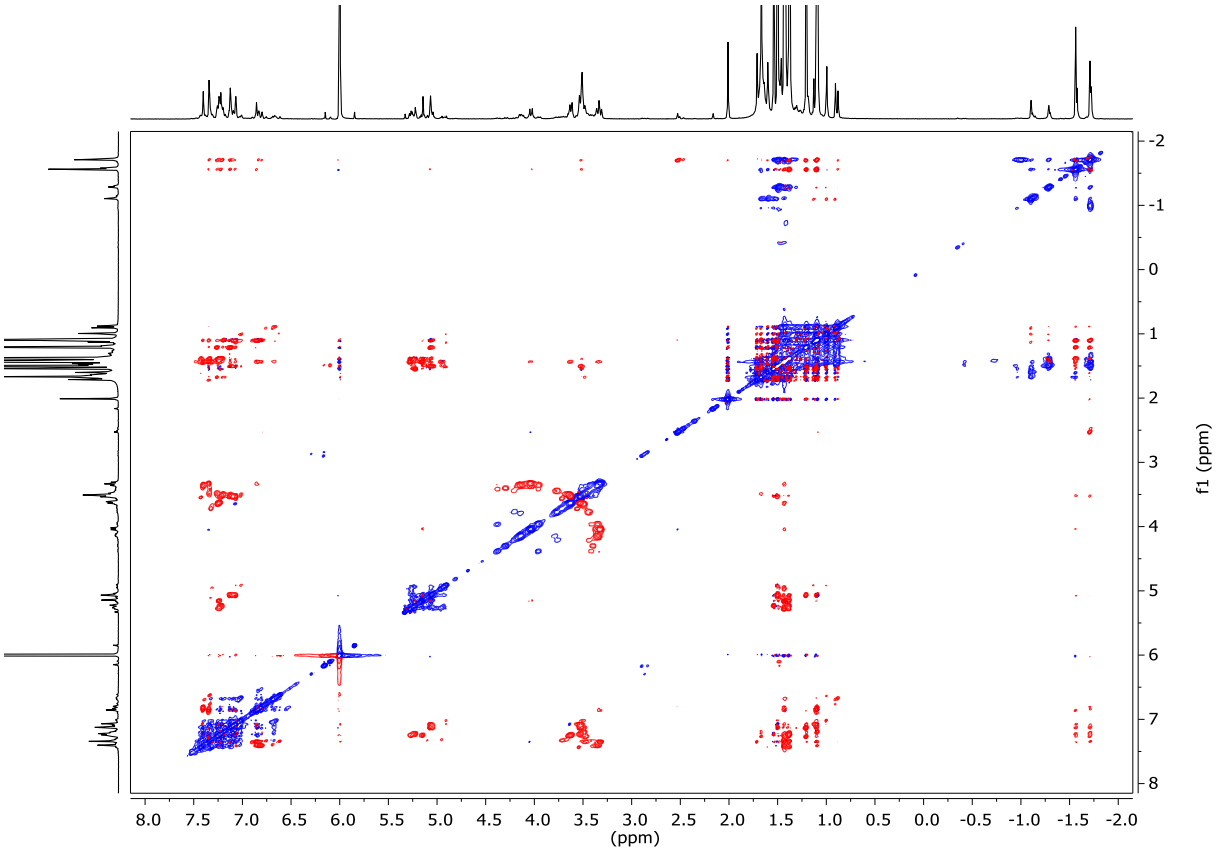

Figure S6: Symmetrized ROESY spectrum of **4** (τ_m: 400 ms, 600 MHz, $(CDCl_2)_2$, 298 K). NOE correlations are in red. EXSY correlations are in blue.

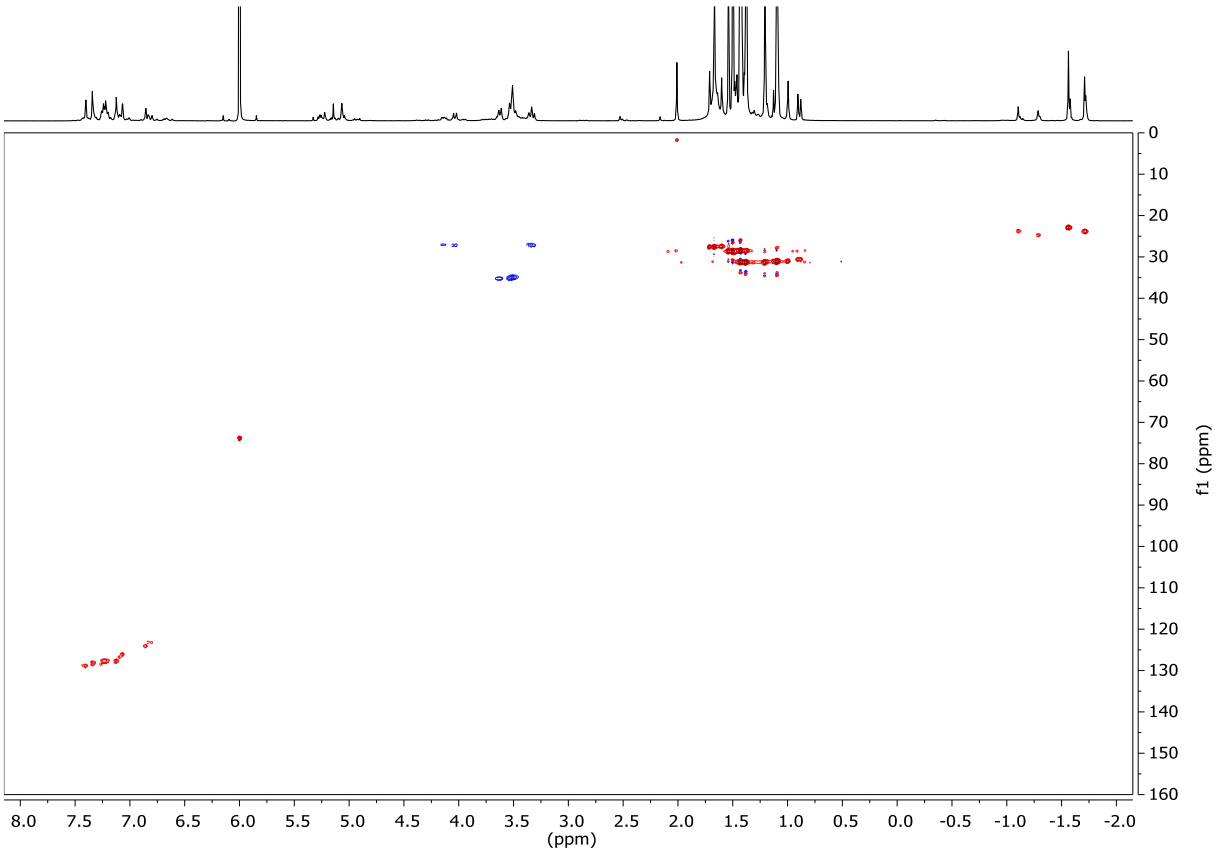

Figure S7: Edited ^{1}H-^{13}C HSQC spectrum of **4** (14.1 Tesla, $(CDCl_2)_2$, 298 K).

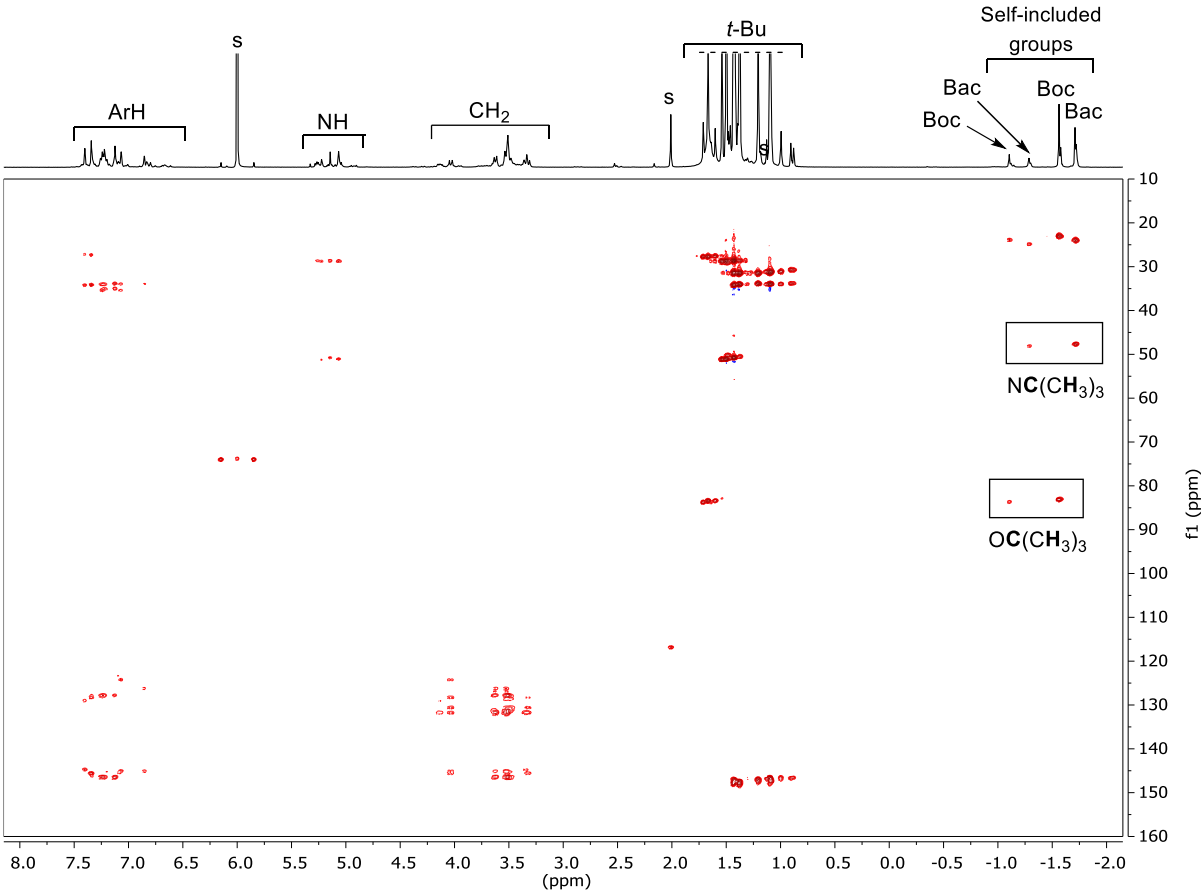

Figure S8: ^{1}H-^{13}C HMBC spectrum of **4** (8 Hz, 14.1 Tesla, $(CDCl_2)_2$, 298 K).

p-*t*Bu-calix[6]arene-mono-acetyl-penta-Bac **5**

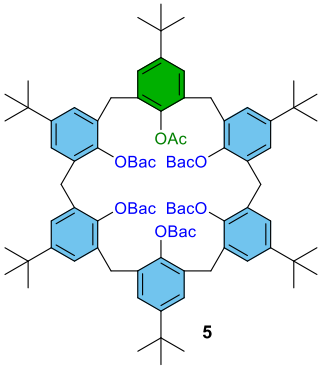

Compared to **1** and **4**, **5** is more soluble in chlorinated solvents such as 1,1,2,2-tetrachloroethane, dichloromethane and chloroform (*e.g.* solubilities of <1 mg/mL, <1mg/mL, and >20 mg/mL for **1**, **4**, and **5**, respectively). The ^{1}H NMR spectra of molecular container **5** also reveals the coexistence of multiple conformers in slow exchange on the chemical shift time scale. The spectrum recorded in $(CDCl_2)_2$ (*i.e.* solvent too big to fit inside this molecular container cavity) shows mainly conformers of **5** self-including one Ac or, in smaller proportions, one Bac group (see HSQC and HMBC, Figures S12-S13). In contrast, the spectrum recorded in the smaller solvent $CDCl_3$ shows almost no trace of Bac group self-inclusion. The 2D-ROESY spectrum recorded in $(CDCl_2)_2$ show numerous EXSY-type correlations proving the presence of several conformers of a single species (Figure S11).

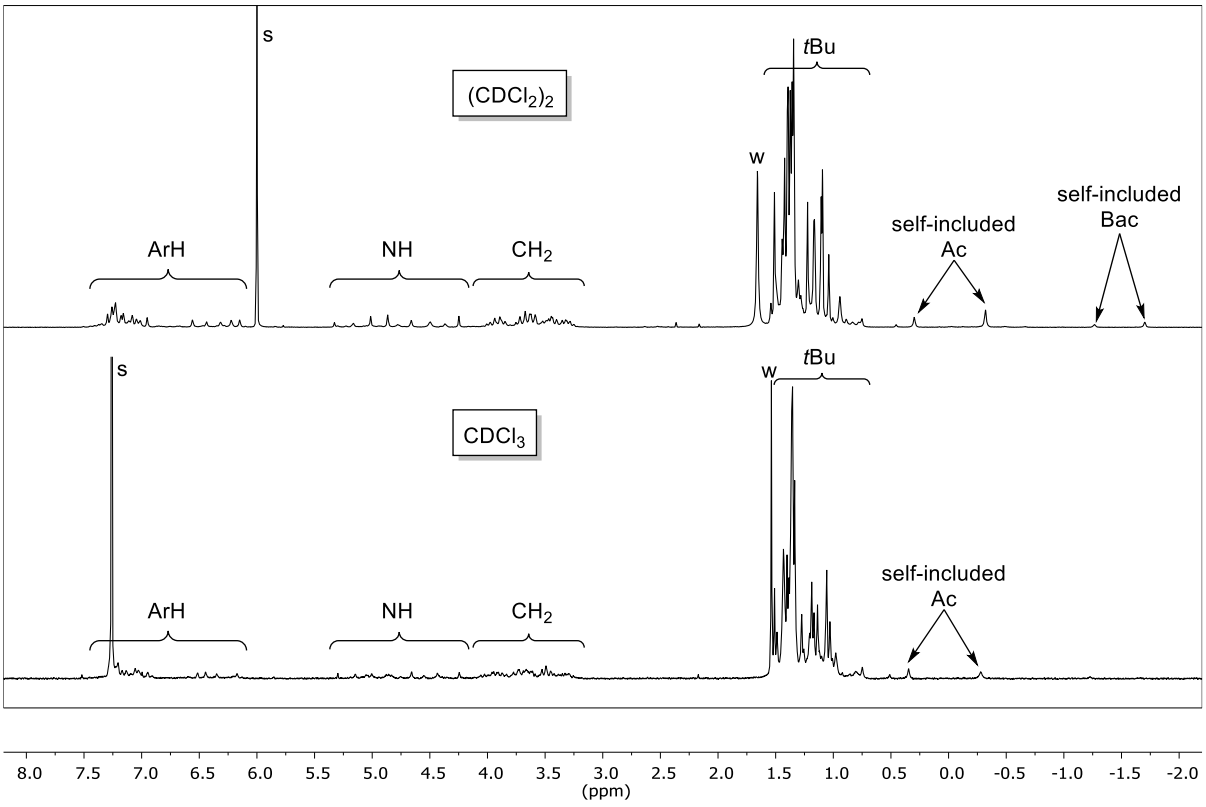

Figure S9. ^{1}H NMR spectra of **5** (Top: 400 MHz, $(CDCl_2)_2$, 298 K; Bottom: 400 MHz, $CDCl_3$, 298 K). s: residual solvent, w: water.

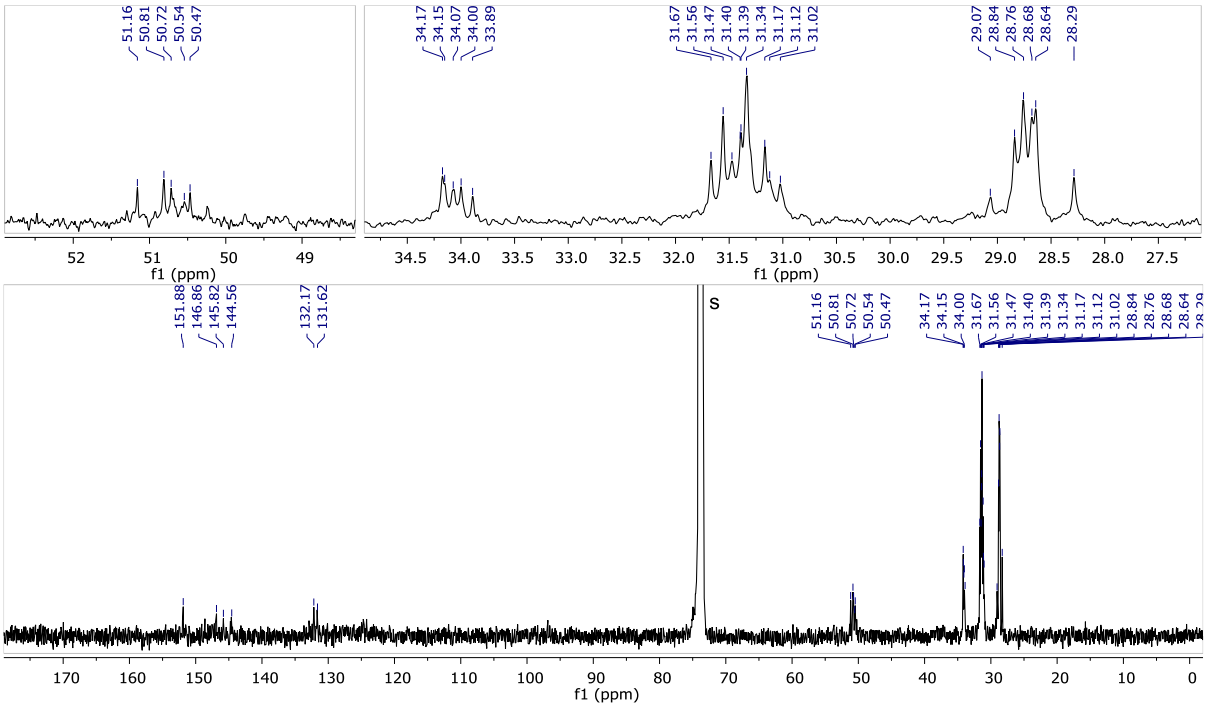

Figure S10. ^{13}C NMR spectra of **5** (100 MHz, $(CDCl_2)_2$, 298 K). s: residual solvent. Only few peaks are observed despite extensive signal averaging (*i.e.* 30000 scans) due to the presence of multiple conformers in slow exchange rate on the NMR chemical shift time scale. The following partial assignment relies on HSQC and HMBC spectra: Ar (120~155 ppm), N-**C** (~50 ppm), Ar-**C**H$_2$-Ar (28~36 ppm), Ar-**C**-CH$_3$ (~34 ppm), Ar-C-**C**H$_3$ (~31 ppm), N-C-**C**H$_3$ (~28 ppm). These data are in agreement with the ^{13}C chemical shifts reported for similar compounds.[1,2,3]

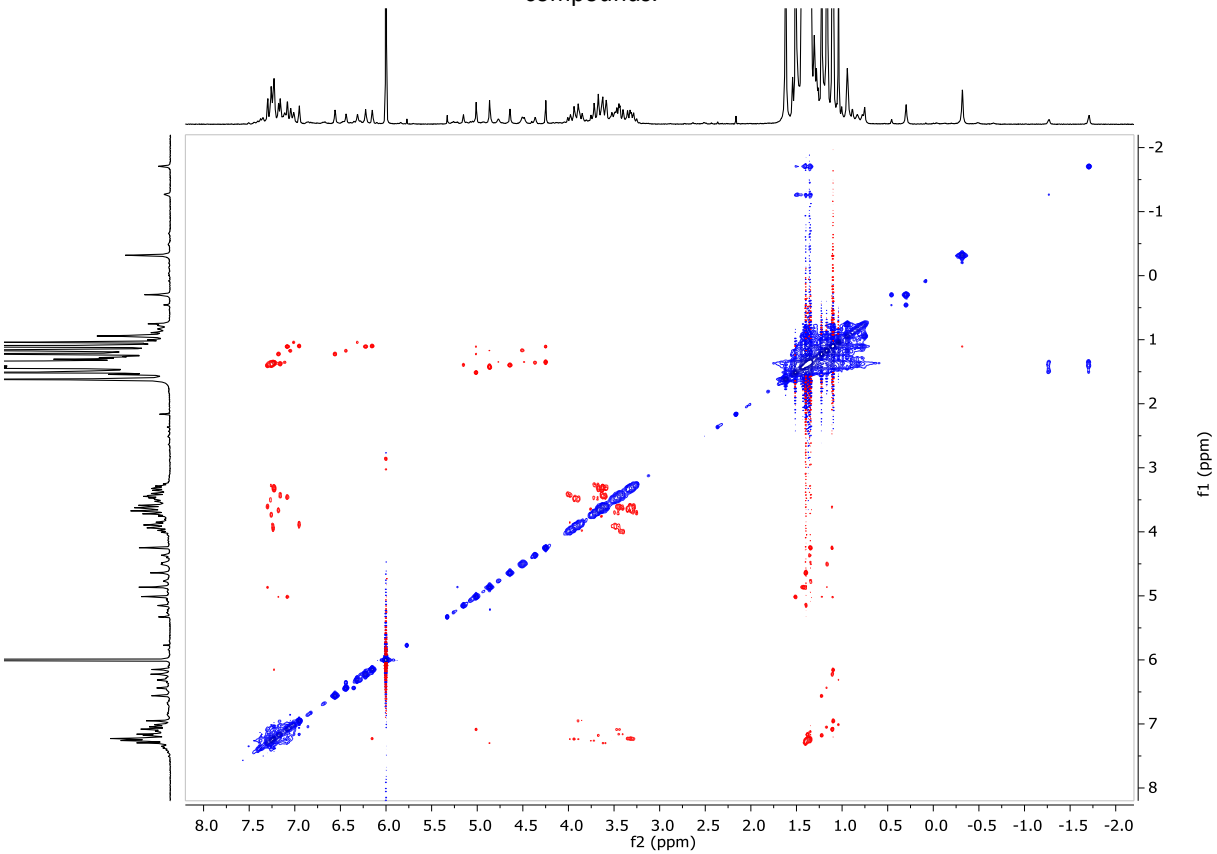

Figure S11: Symmetrized ROESY spectrum of **5** (τ_m: 400 ms, 400 MHz, $(CDCl_2)_2$, 298 K). NOE correlations are in red. EXSY correlations are in blue.

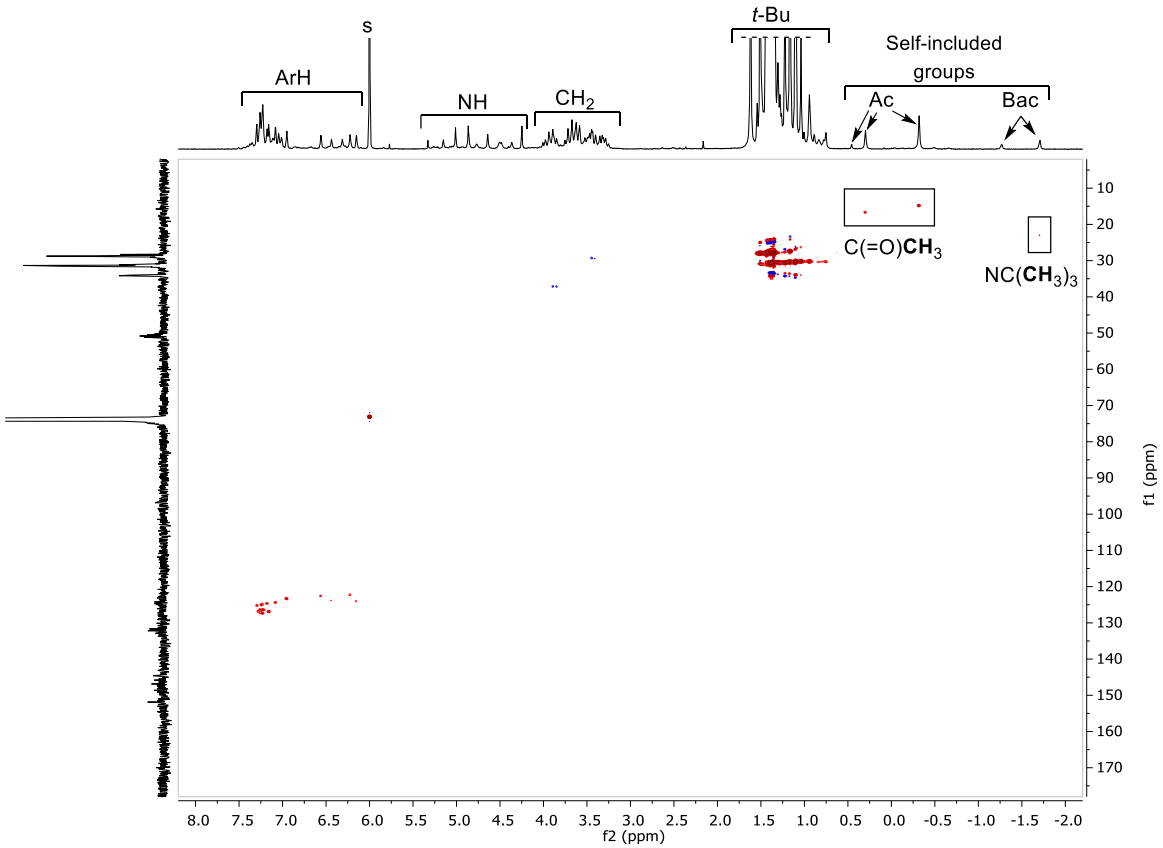

Figure S12: Edited ^{1}H-^{13}C HSQC spectrum of **5** (9.4 Tesla, $(CDCl_2)_2$, 298 K).

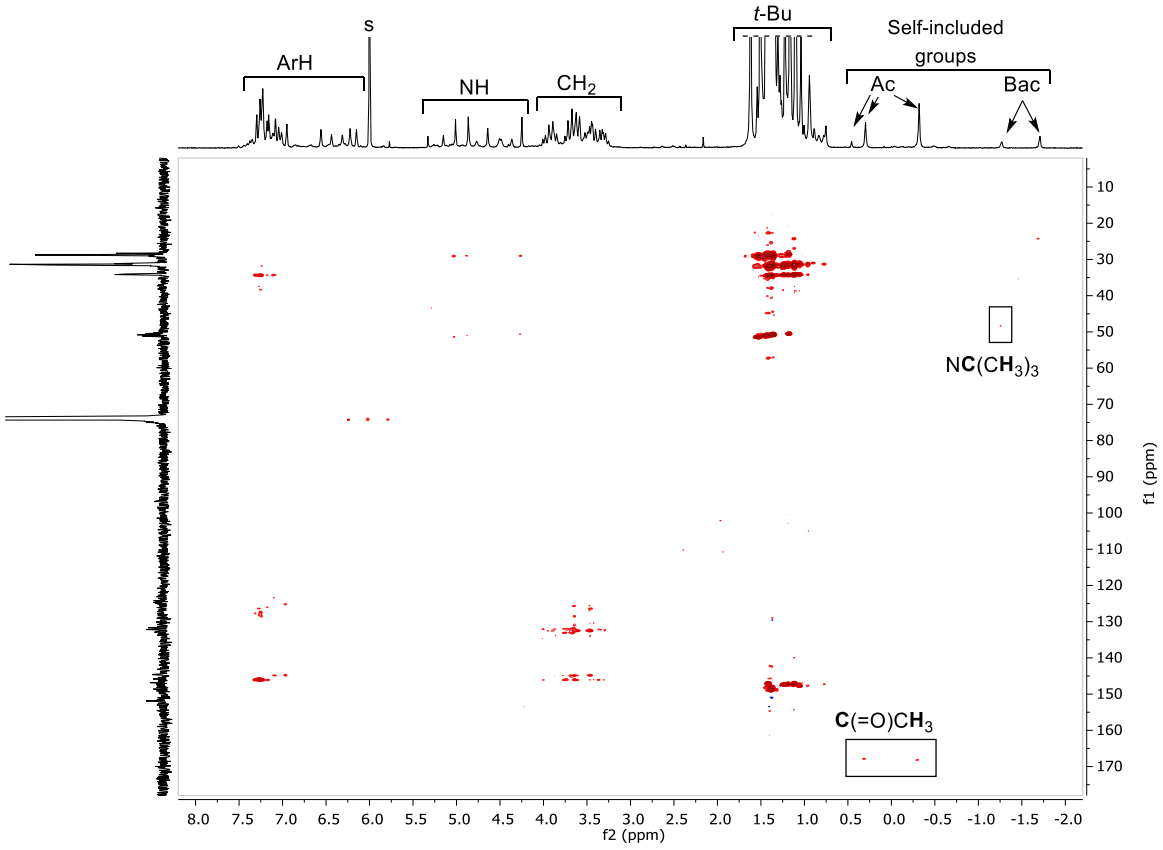

Figure S13: ^{1}H-^{13}C HMBC spectrum of **5** (8 Hz, 9.4 Tesla, $(CDCl_2)_2$, 298 K).

Solution-state host–guest studies

Association constants determination

For all of the systems under study, the in-out guest exchange at 298 K is a slow process on the NMR chemical shift time scale and the association constants (K_a) were thus determined by integration of suitable ^{1}H or ^{19}F NMR signals pertaining to the free host (H_{free}), free guest (G_{out}) and to the corresponding 1:1 host–guest inclusion complex (HG). Considering signal overlapping the following integrals were used:

- aromatic region of the ^{1}H spectrum accounting for the total concentration of host (H_{tot}, 12 Hydrogens);
- signal(s) of the included guest (G_{in}), which are observed at high-field due to ring-current effects originating from the polyaromatic walls of the host cavity, accounting for the concentration of the complex;
- signal of free guest (G_{out}).

In some cases, the signal of G_{out} overlapped with signals of the methylene bridges of the host ($ArCH_2Ar$). The integral corresponding to the free guest was then determined by subtracting the value expected for the $ArCH_2Ar$ signals (12 H), as determined by integration of the aromatic region, to the total integral of the overlapping G_{out} and $ArCH_2Ar$ signals.

The K_a was calculated according to the following formula:

$$K_a = \frac{[\mathrm{HG}]}{[\mathrm{H_{free}}] \times [\mathrm{G_{out}}]} = \frac{[\mathrm{G_{in}}]}{([\mathrm{H_{tot}}] - [\mathrm{G_{in}}]) \times [\mathrm{G_{out}}]}$$

The K_a data provided in Table 1 of the manuscript are averaged values determined at various concentrations of the guest (except in the cases of Imi@**4** and SF_6@**4**). The relative standard deviations were below 20% in all cases.

Study of **1**–$(CH_2Cl)_2$ host–guest system

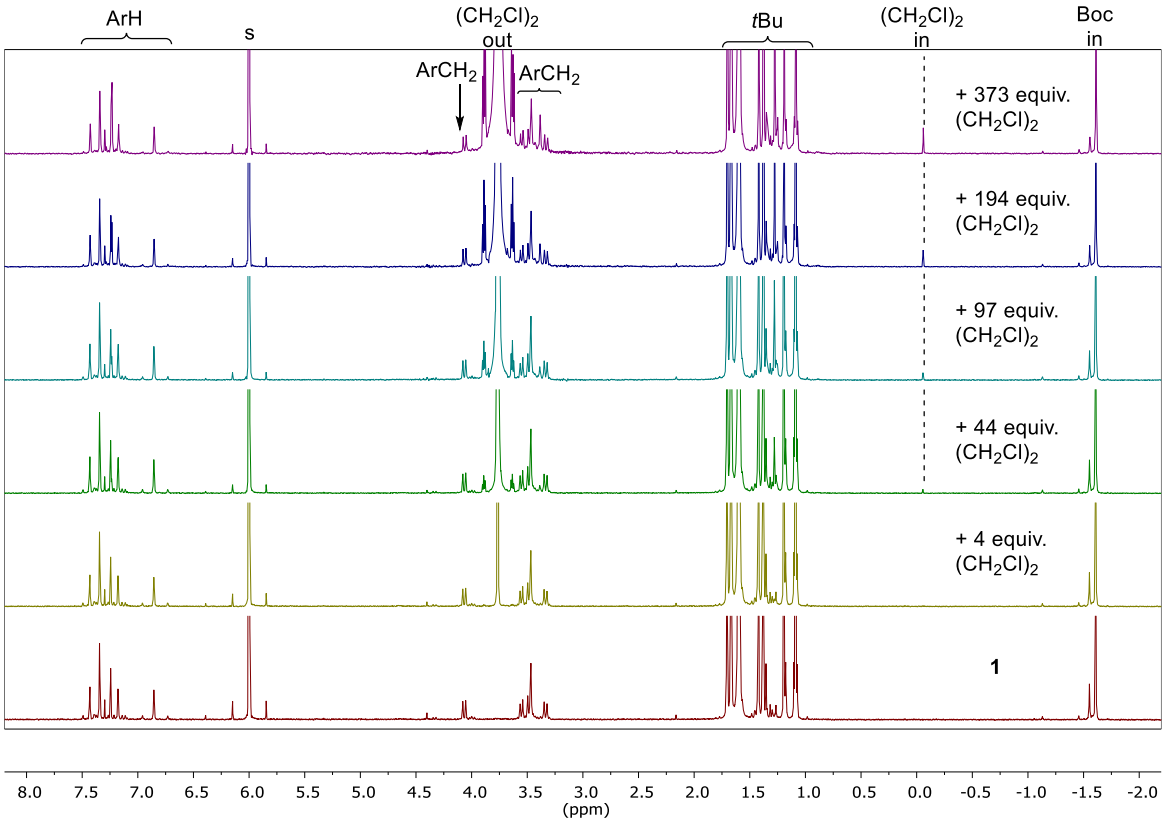

Figure S14. ^{1}H NMR spectra (600 MHz, $(CDCl_2)_2$, 298 K) of **1** before and after addition of variable amounts of $(CH_2Cl)_2$. s: residual solvent.

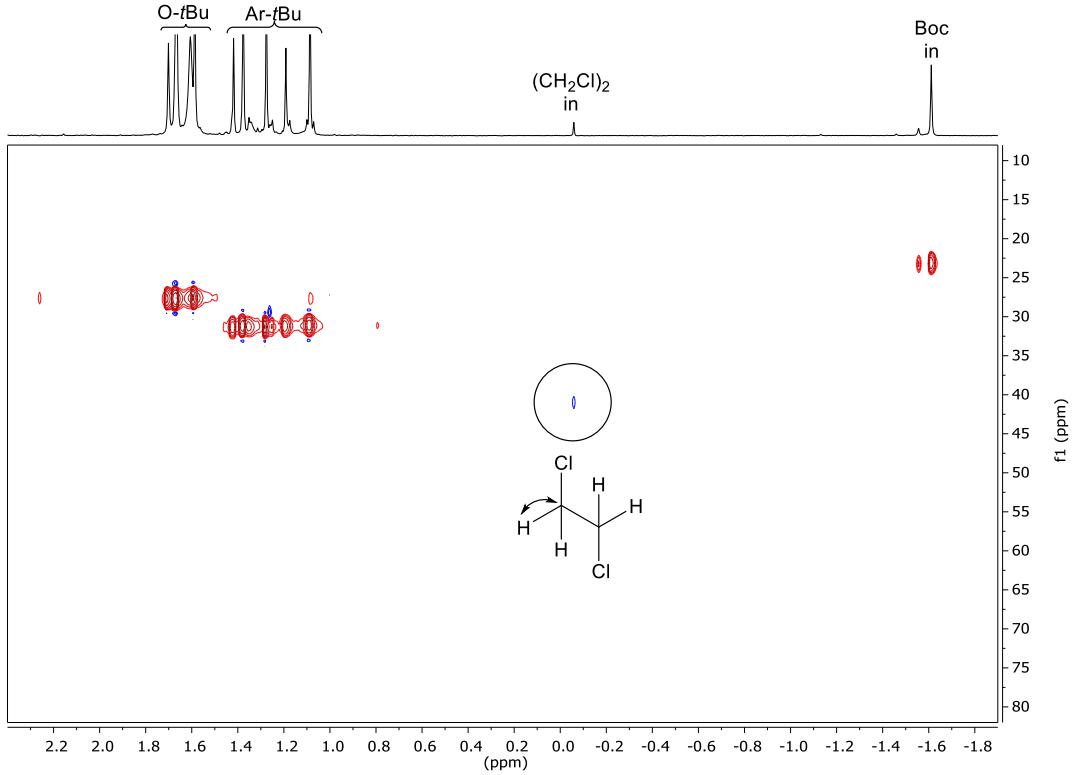

Figure S15: Region of the edited ^{1}H-^{13}C HSQC spectrum of **1** in presence of 373 equiv. of $(CH_2Cl)_2$ (14.1 Tesla, $(CDCl_2)_2$, 298 K). Negative correlations (methylenes) are in blue.

Study of **1**–Imi host–guest system

No inclusion complex could be detected upon addition of 21 equiv. of Imi in $(CDCl_2)_2$.

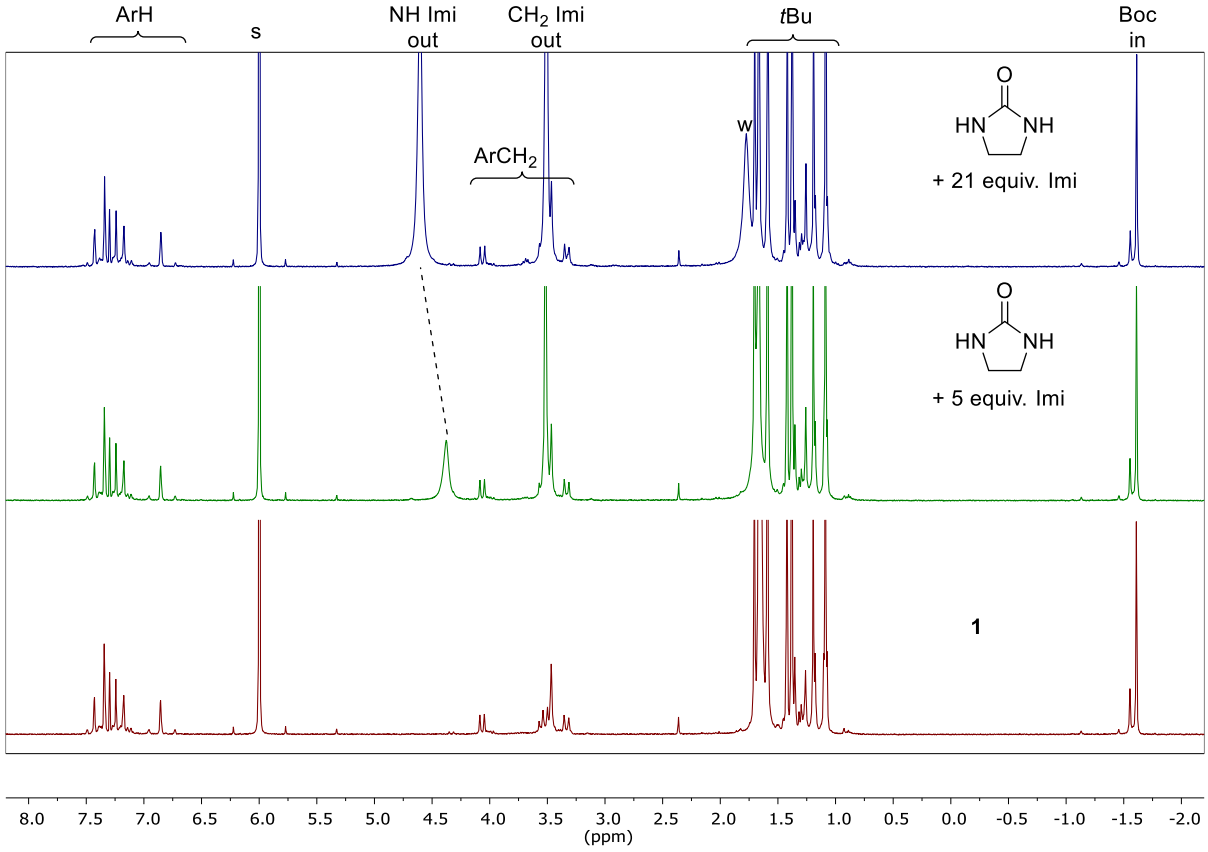

Figure S16. ^{1}H NMR spectra (400 MHz, $(CDCl_2)_2$, 298 K) of **1** before and after addition of variable amounts of Imi. s: residual solvent, w: water.

Study of **4**–$(CH_2Cl)_2$ host–guest system

In contrast to the complex $(CH_2Cl)_2$@**1**, for which a single signal was observed for the included guest, four peaks of variable intensities are observed for $(CH_2Cl)_2$ in the complex $(CH_2Cl)_2$@**4** (see 1D-Exsy spectrum of Figure S18). The complexation induced shifts (CIS) are -2.61 (hidden signal in the *t*Bu region), -3.22, -3.24 and -3.78 ppm. This can be explained by the formation of several complexes differing by the conformation of the calixarenic skeleton and/or by the diastereotopicity of the included guest hydrogen atoms.

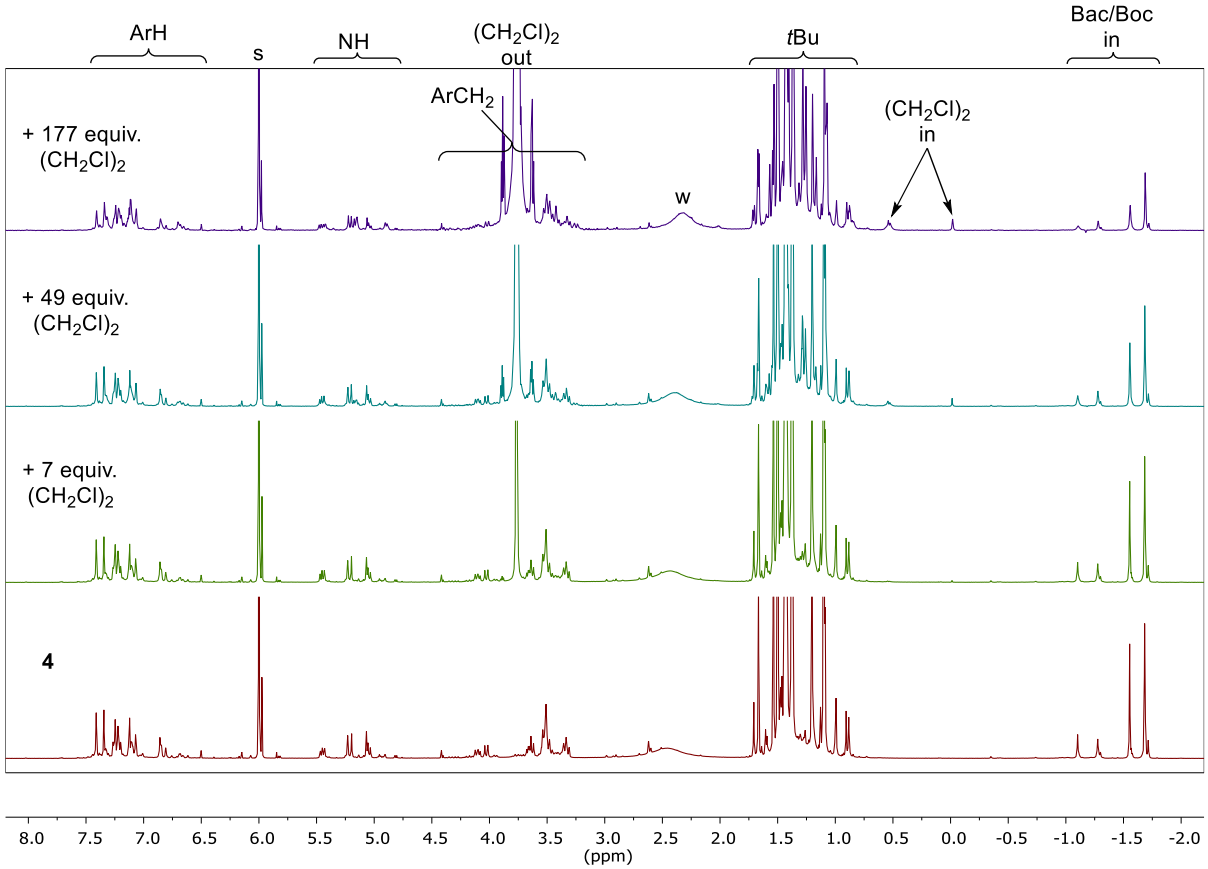

Figure S17. ^{1}H NMR spectra (600 MHz, $(CDCl_2)_2$, 298 K) of **4** before and after addition of variable amounts of $(CH_2Cl)_2$. s: residual solvent, w: water.

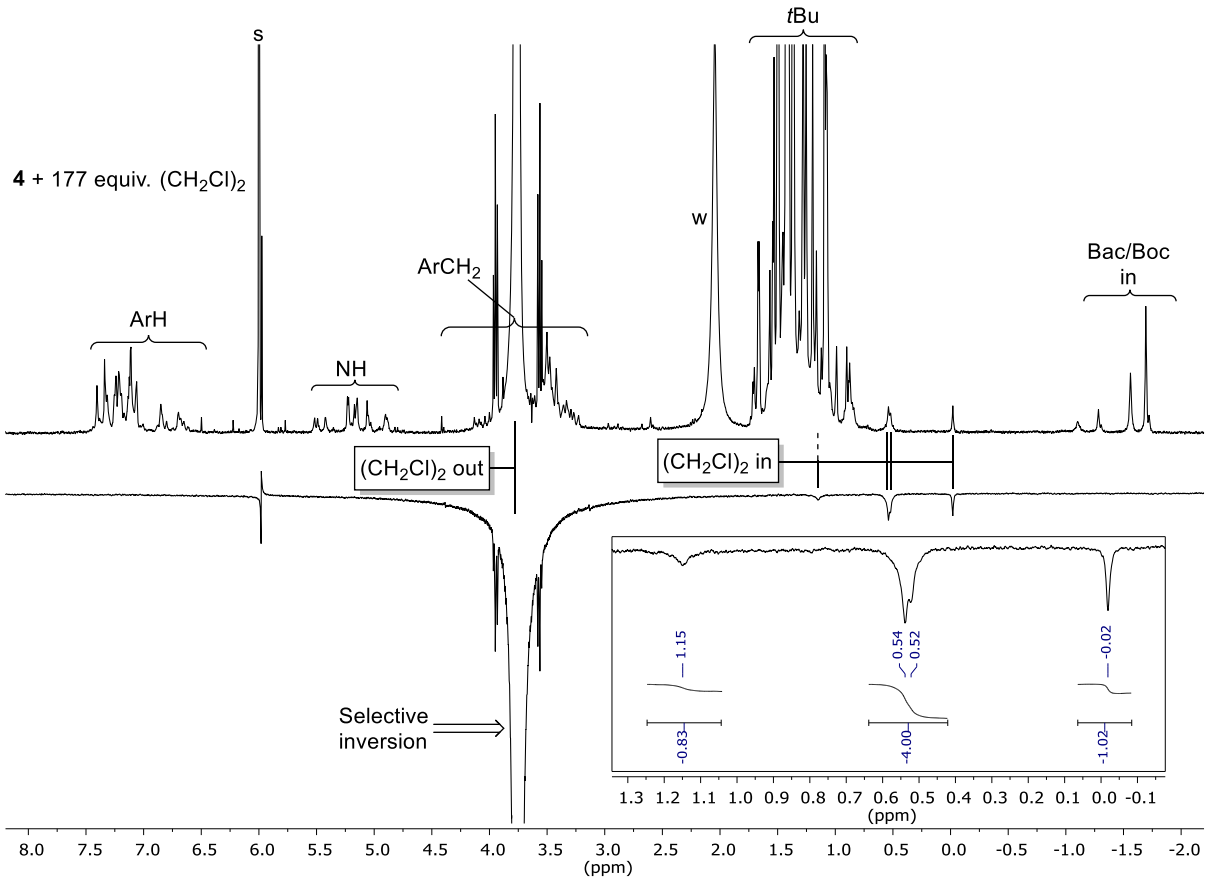

Figure S18. Top: ^{1}H NMR spectrum (400 MHz, $(CDCl_2)_2$, 298 K) of **4** with an excess of $(CH_2Cl)_2$. Bottom: 1D-ROESY spectrum (τ_m = 200 ms, 400 MHz, $(CDCl_2)_2$, 298 K, selective inversion at 3.79 ppm ± 50 Hz). s: residual solvent, w: water.

Study of **4**–Imi host–guest system

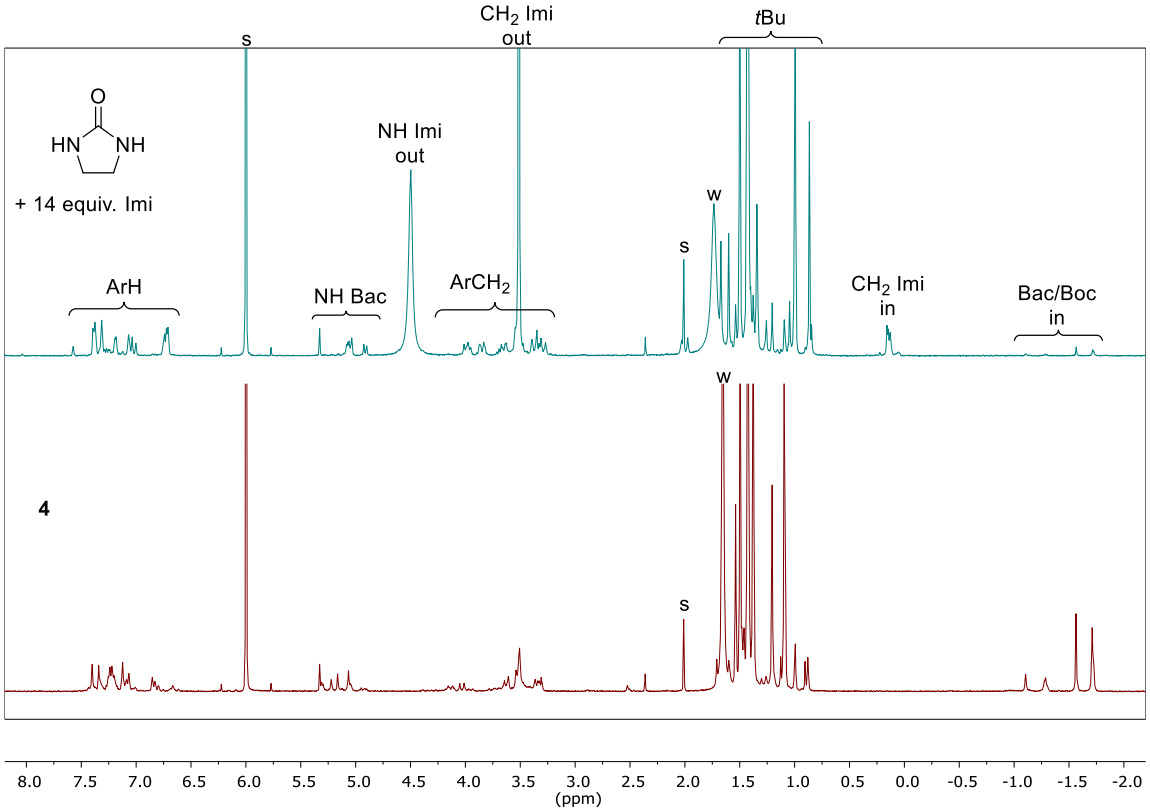

Figure S19. ^{1}H NMR spectra (400 MHz, $(CDCl_2)_2$, 298 K) of **4** before and after addition of an excess of Imi. s: residual solvents, w: water.

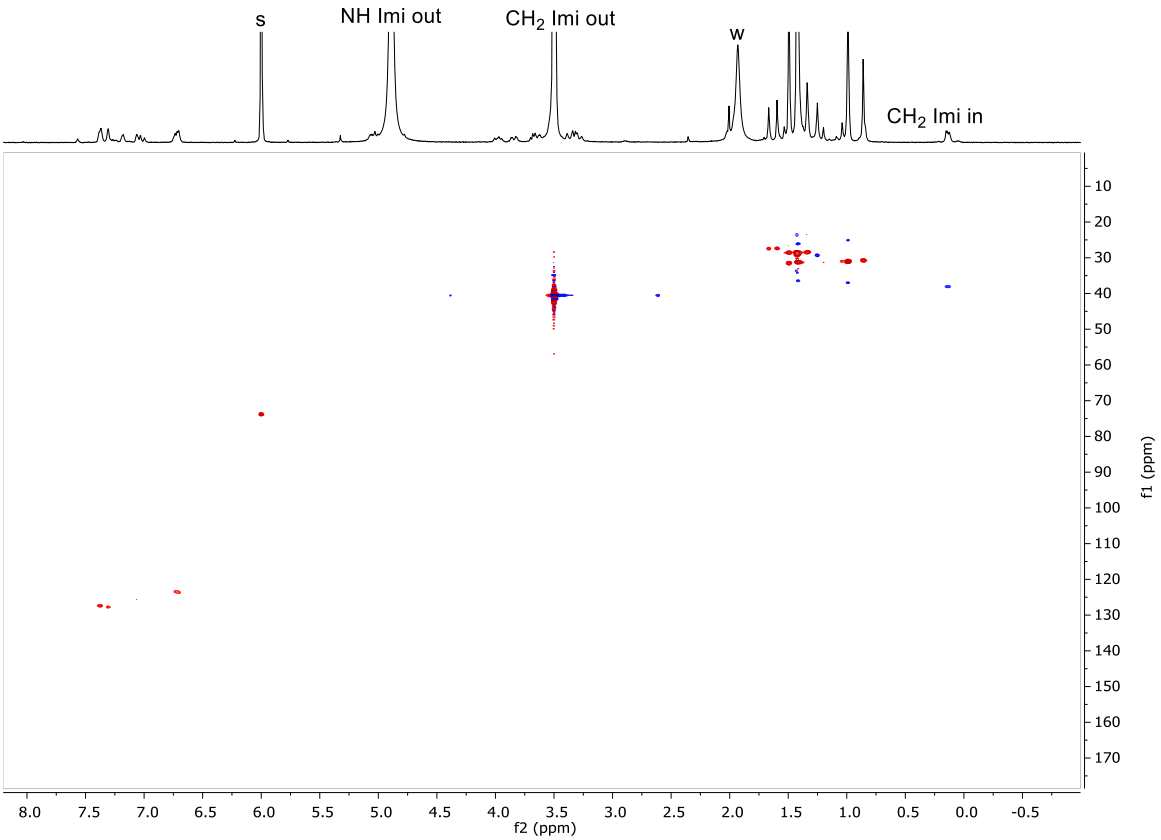

Figure S20: Edited ^{1}H-^{13}C HSQC spectrum of **4** in presence of an excess of Imi (9.4 Tesla, $(CDCl_2)_2$, 298 K). Negative correlations (methylenes) are in blue. s: residual solvent, w: water.

Study of **4**–DMSO host–guest system

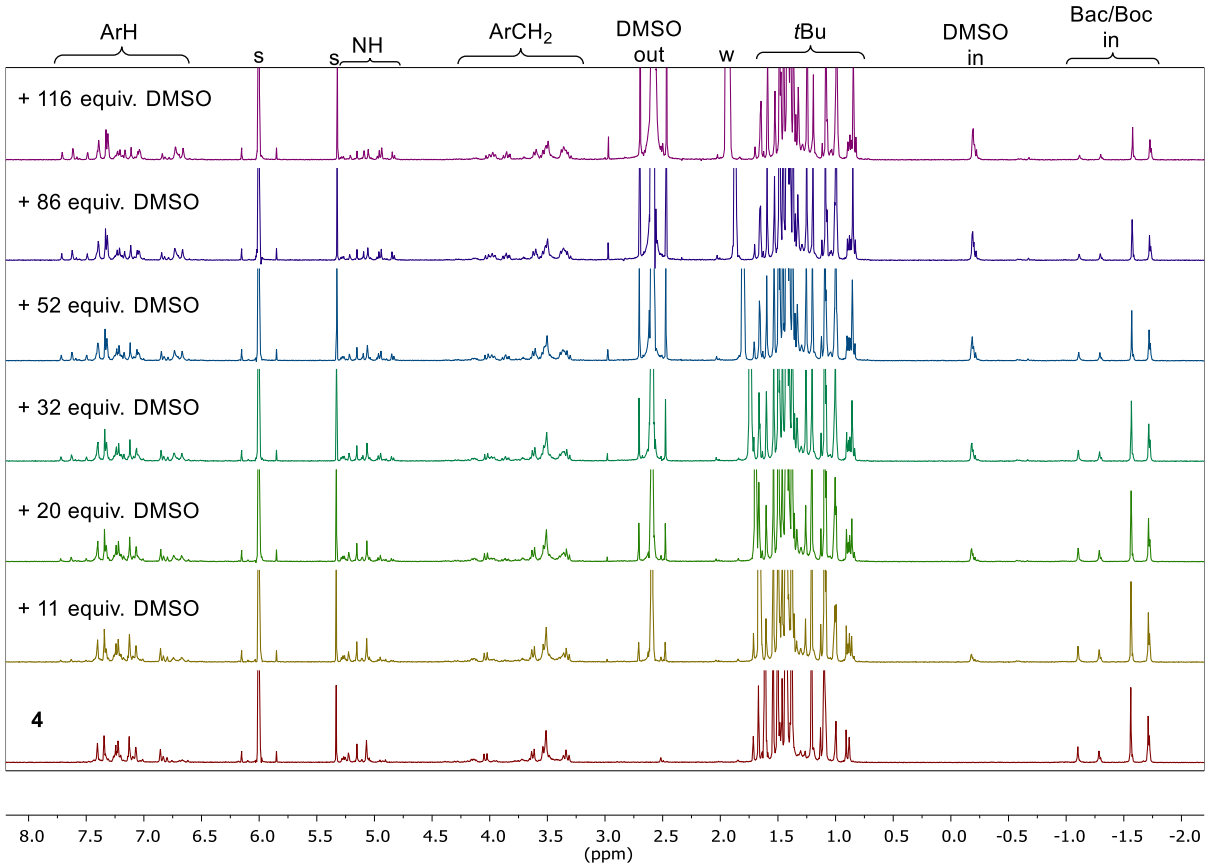

Figure S21. ^{1}H NMR spectra (600 MHz, $(CDCl_2)_2$, 298 K) of **4** before and after addition of variable amounts of DMSO. s: residual solvents, w: water.

Study of **4**–CS_2 host–guest system

No inclusion complex could be detected upon addition of a large excess of CS_2 to a solution of **4** in $(CDCl_2)_2$. Decreasing intensities are observed upon addition of CS_2 due to dilution.

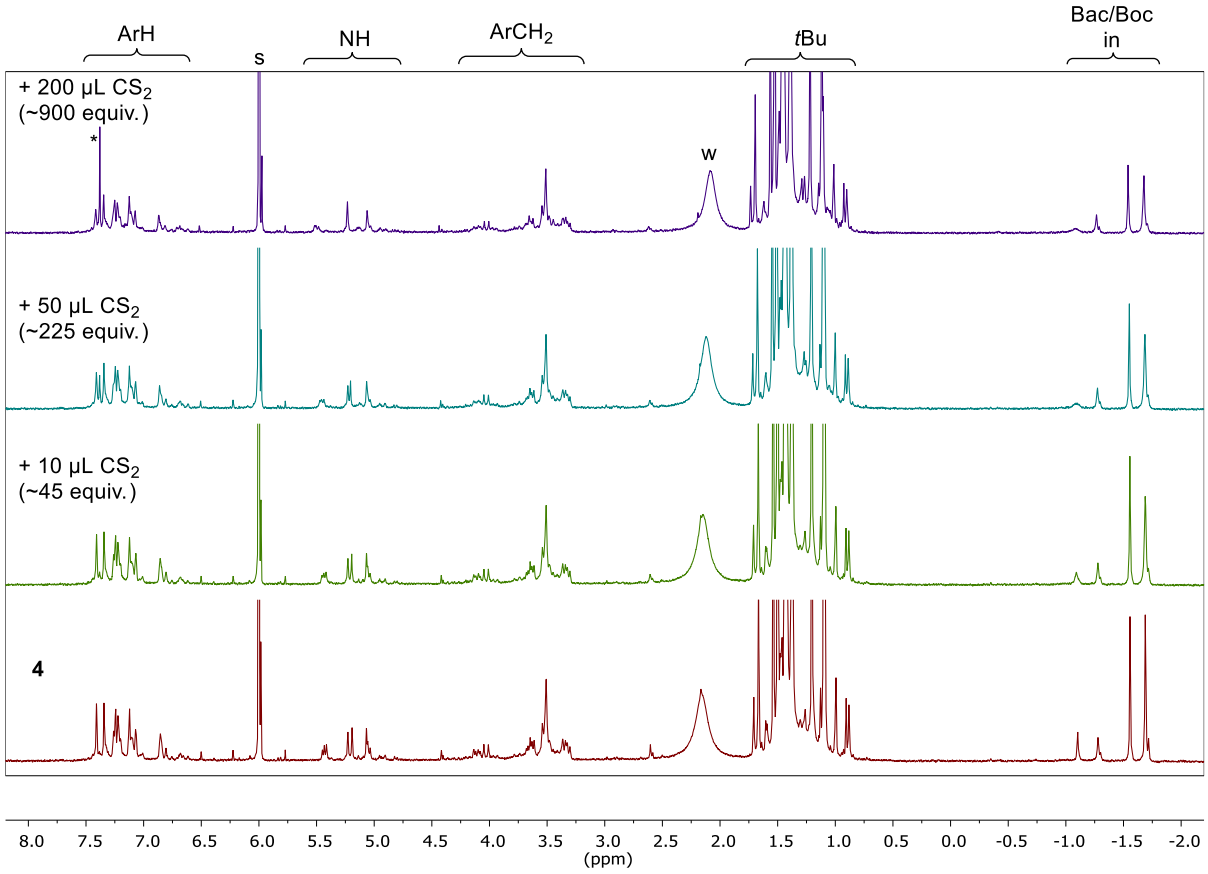

Figure S22. ^{1}H NMR spectra (400 MHz, $(CDCl_2)_2$, 298 K) of **4** before and after addition of variable amounts of CS_2. s: residual solvent, w: water, *: impurity contained in CS_2.

Study of **4**–CO_2 host–guest system

In order to monitor the possible formation of a CO_2@**4** inclusion complex in solution, we recorded spectra of **4** in $(CDCl_2)_2$ under a ~11.5 bar pressure of $^{13}CO_2$ (99.2% ^{13}C-labelled carbon dioxide gas purchased from Eurisotop). No ^{13}C NMR signal ascribable to an inclusion complex was detected (signal expected to be high-field shifted by a few ppm with respect to the signal of free CO_2 as a consequence of ring current effects due to the polyaromatic walls of the cavity). No significant change of the ^1H spectrum was detected in the presence of CO_2.

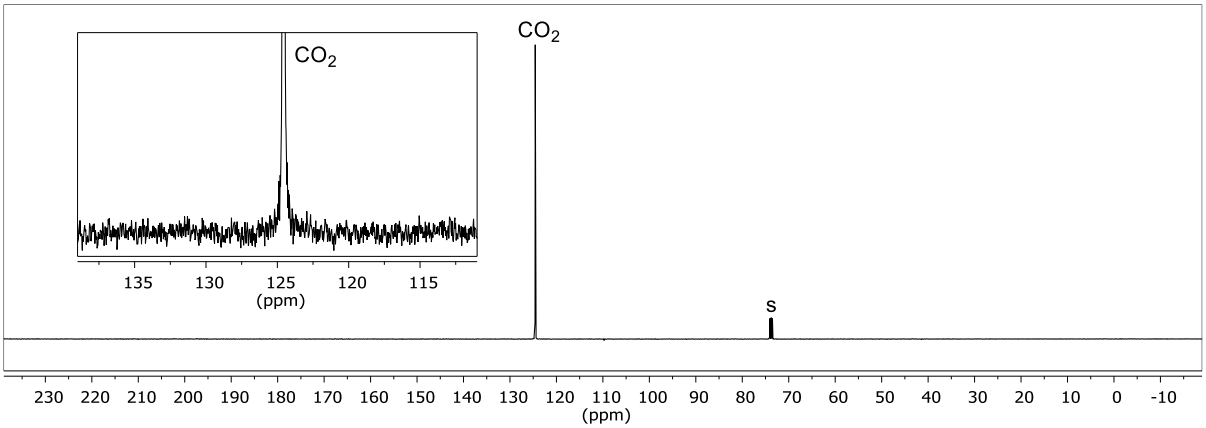

Figure S23. ^{13}C NMR spectrum (100 MHz, $(CDCl_2)_2$, 298 K) of **4** in presence of an excess of $^{13}CO_2$ (11.5 bar). s: solvent.

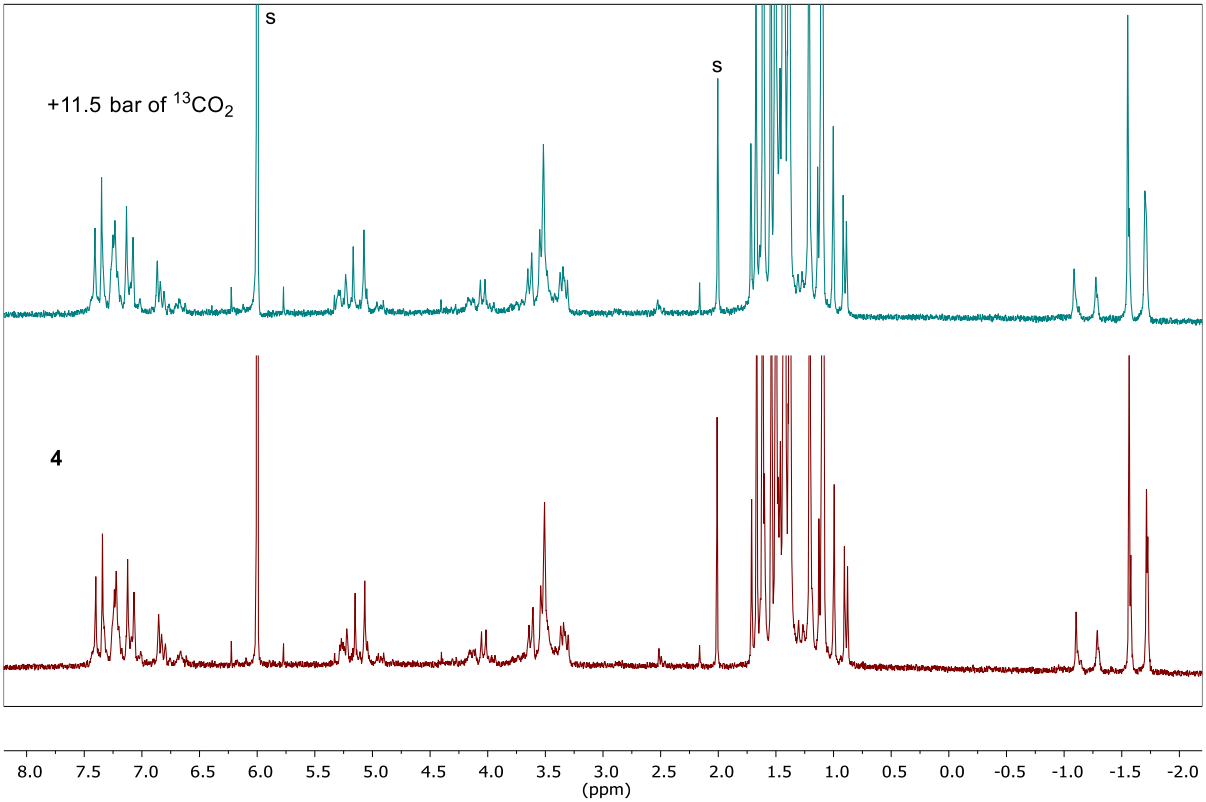

Figure S24. ^1H NMR spectra (400 MHz, $(CDCl_2)_2$, 298 K) of **4** under air and under a 11.5 bar pressure of $^{13}CO_2$. s: residual solvents.

Study of **4**–SF_6 host–guest system

In order to monitor the possible formation of a SF_6@**4** inclusion complex in solution, we recorded spectra of **4** in $(CDCl_2)_2$ under a ~8 bar pressure of SF_6. The ^{19}F NMR revealed several high-field shifted weak signals that were assigned to SF_6 included in different conformers of **4** (complexation induced shift = -3.6~4.7 ppm). The concentrations of free and included SF_6 were determined through quantitative ^{19}F NMR using an external standard ($[SF_6]_{out}$ = 0.105 M ; $[SF_6]_{in}$ = 7.47 × 10^{-5} M ; $[\mathbf{4}]_{tot}$ = 4.16 × 10^{-3} M). In accordance with the extremely small association constant (*i.e.* 0.2 M^{-1}), no significant change of the ^1H spectrum was detected in the presence of SF_6.

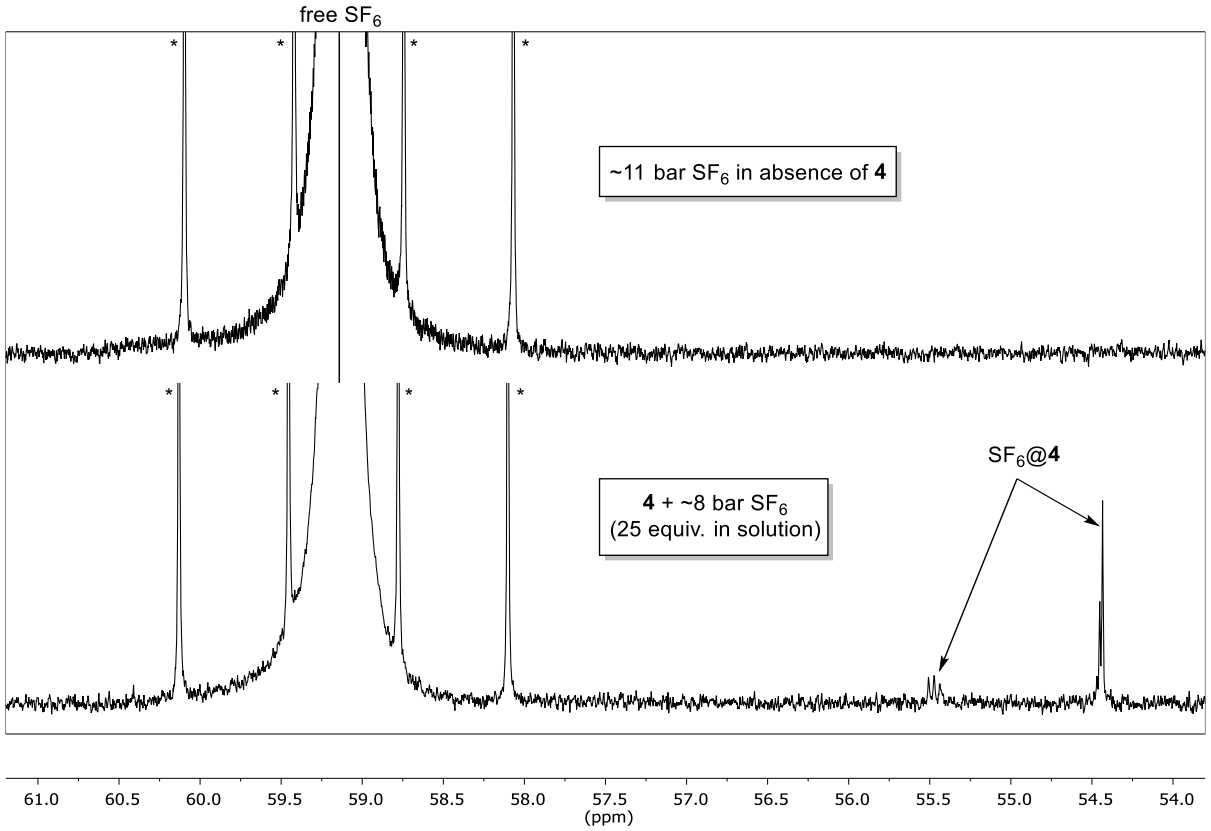

Figure S25. ^{19}F NMR spectra of SF_6 in the absence (top) and presence (bottom) of molecular container **4** (376 MHz, $(CDCl_2)_2$, 298 K). *: ^{33}S satellites.The chemical shift scale was not precisely calibrated.

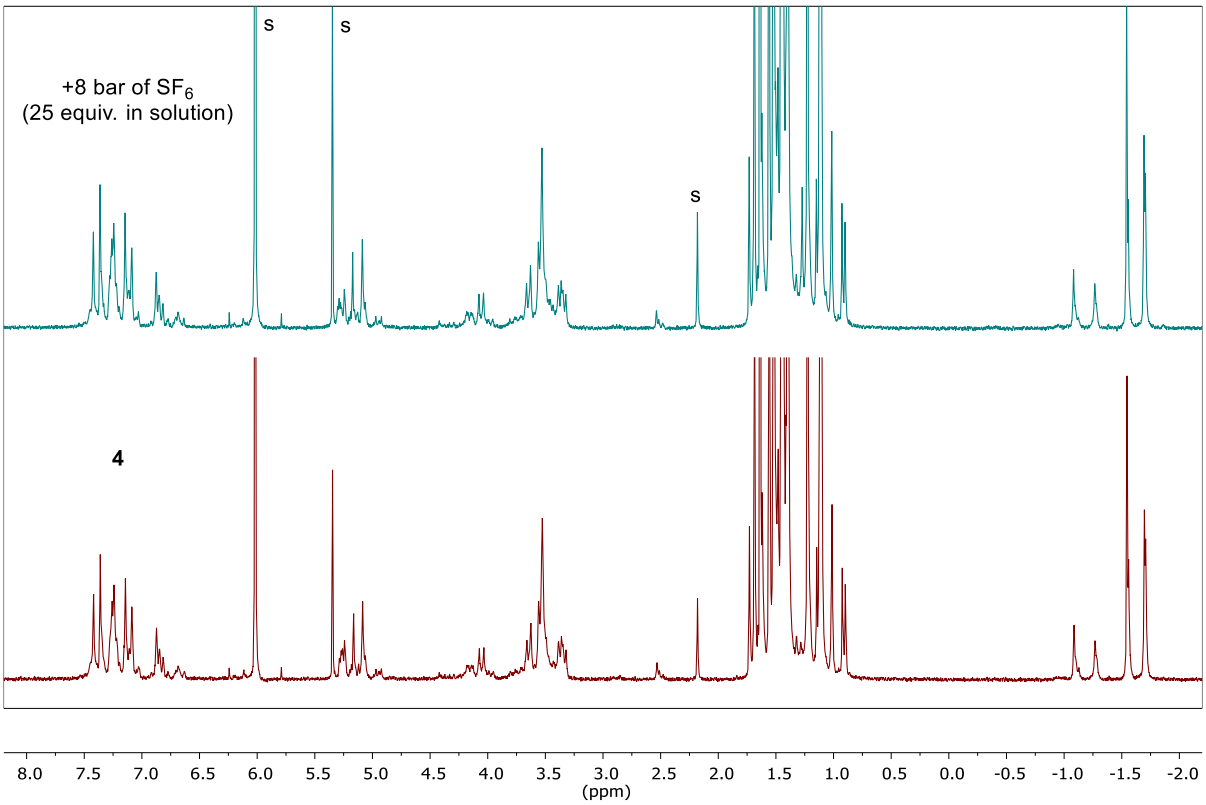

Figure S26. ^{1}H NMR spectra (400 MHz, $(CDCl_2)_2$, 298 K) of **4** under air and under an 8 bar pressure of SF_6. s: residual solvents.

Study of **5**–Imi host–guest system

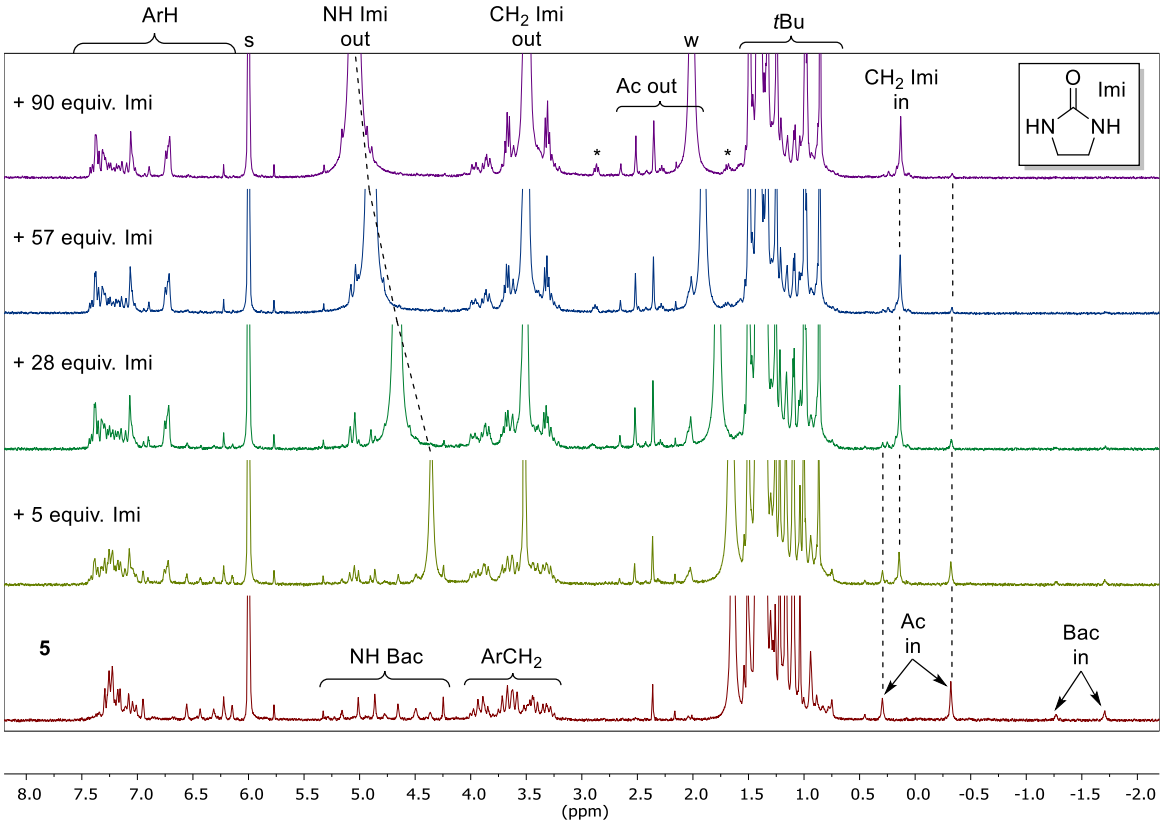

Figure S27. ^{1}H NMR spectra (400 MHz, $(CDCl_2)_2$, 298 K) of **5** before and after addition of variable amounts of Imi. s: residual solvent, w: water, *: impurity from the Imi sample.

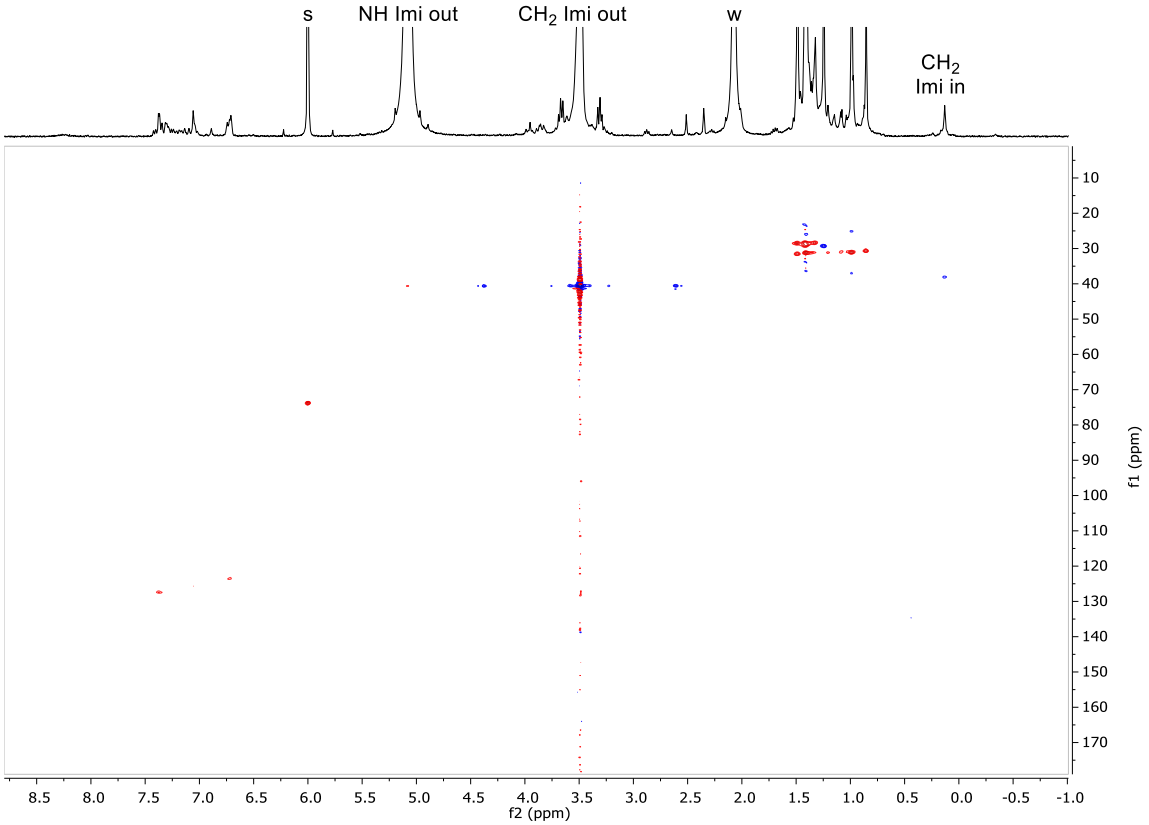

Figure S28: Edited ^{1}H-^{13}C HSQC spectrum of **5** in presence of an excess of Imi (9.4 Tesla, $(CDCl_2)_2$, 298 K). Negative correlations (methylenes) are in blue. s: residual solvent, w: water.

Study of **5**–DMSO host–guest system

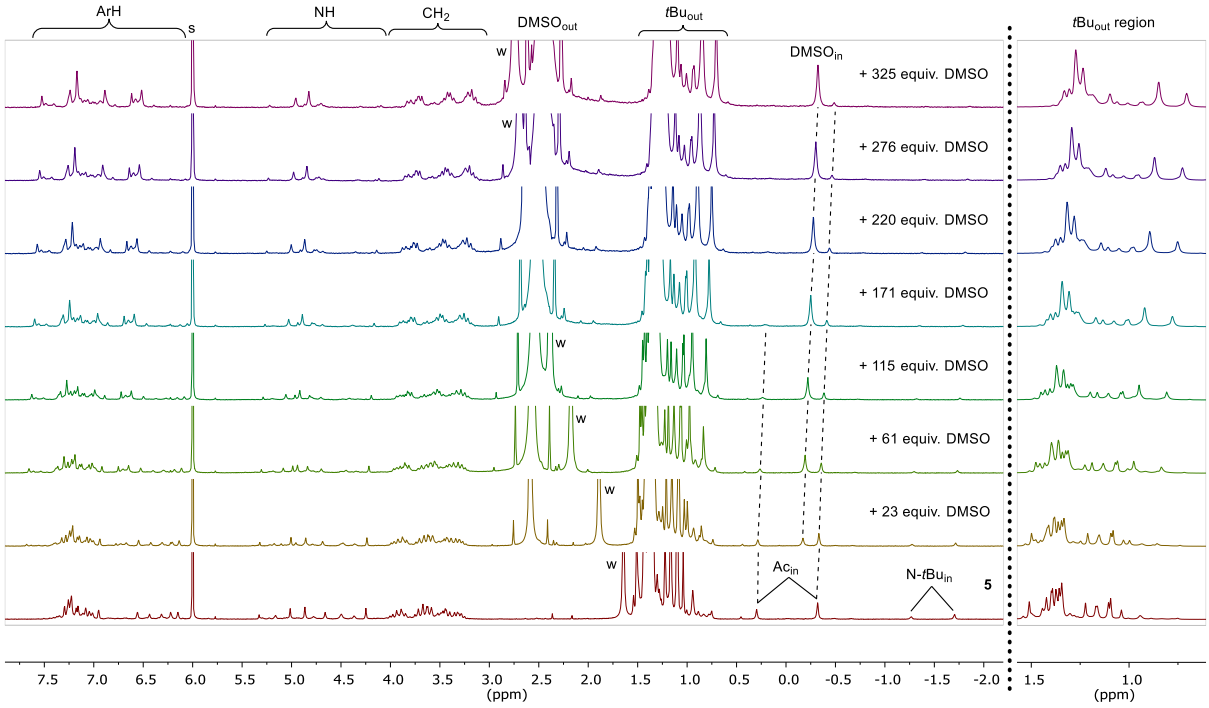

Figure S29. ^{1}H NMR spectra (400 MHz, $(CDCl_2)_2$, 298 K) of **5** before and after addition of variable amounts of DMSO. s: residual solvent, w: water.

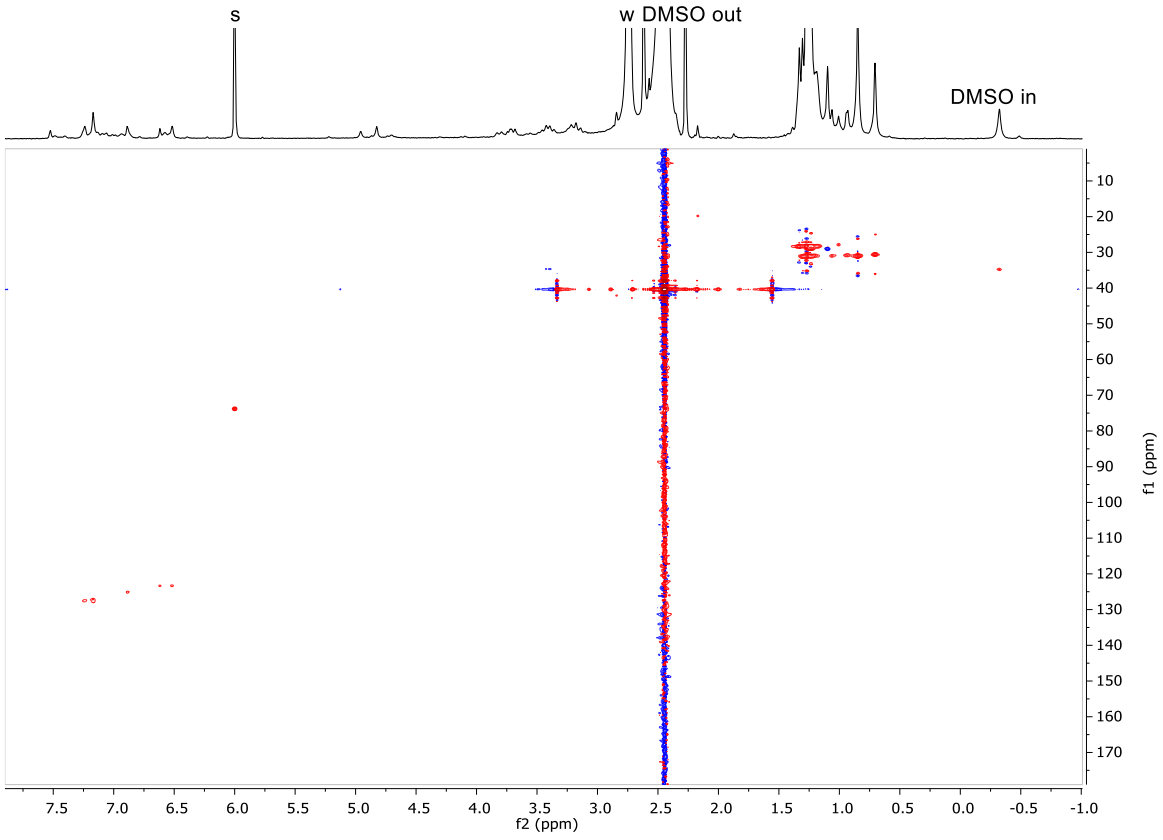

Figure S30: Edited ^{1}H-^{13}C HSQC spectrum of **5** in presence of an excess of DMSO (9.4 Tesla, $(CDCl_2)_2$, 298 K). Negative correlations (methylenes) are in blue. s: residual solvent, w: water.

NMR monitoring of gas release upon dissolution of SF_6@4 crystals

Crystals of SF_6@**4** were dissolved in $(CDCl_2)_2$ for monitoring the gas release in solution. In addition to the experiment described in the manuscript, one experiment was conducted with crystals stored under vacuum (0.1 mbar) at room temperature for 17 hours and showed the same amount of released SF_6 per mg of crystals as using freshly prepared and untreated crystals.

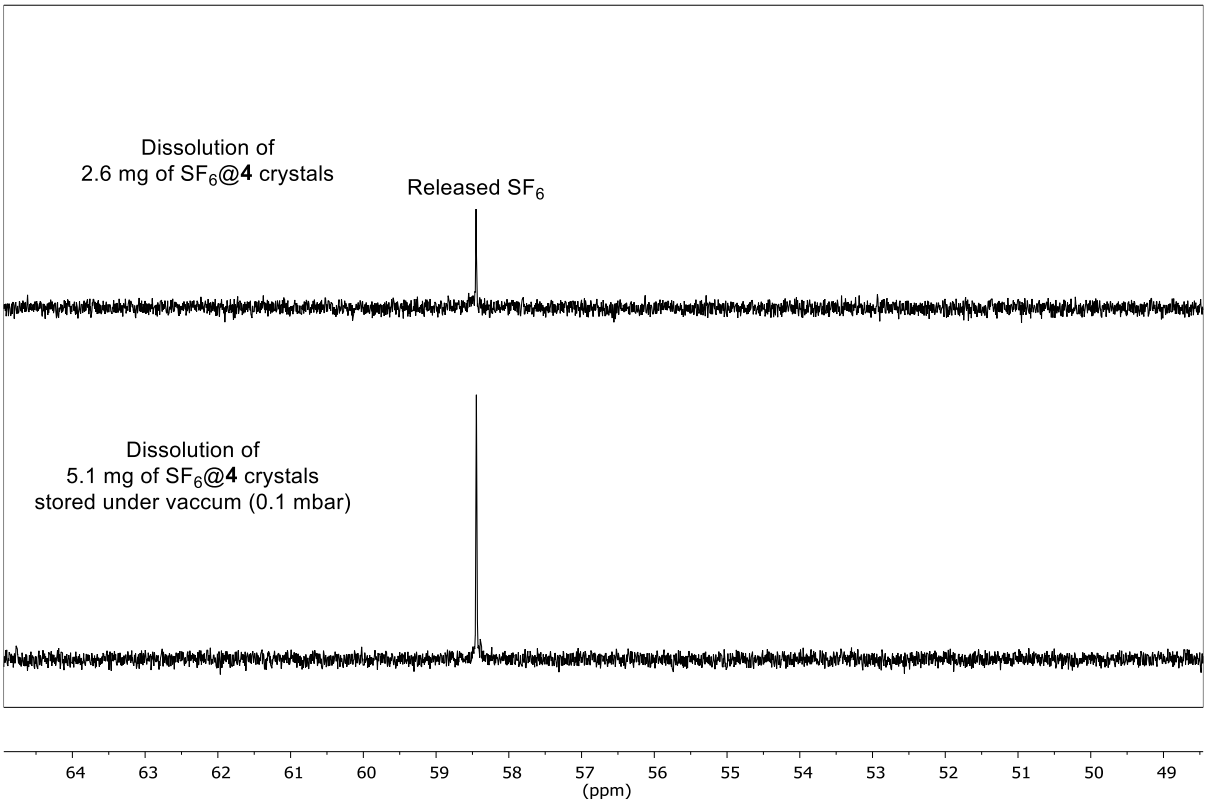

Figure S31. ^{19}F NMR spectra showing the release of SF_6 from SF_6@**4** crystals (376 MHz, $(CDCl_2)_2$, 298 K, 512 scans recorded between about 10 and 35 minutes after dissolution). The crystals were obtained through crystallogenesis method B. Top: freshly prepared and untreated crystals. Bottom: crystals stored under a pressure of 0.1 mbar for 17 hours before dissolution.

Packing in the crystalline state

The three crystal structures of $(CH_2Cl)_2$@**4**, SF_6@**4** and CO_2@**4** display similar packing of the host–guest complexes in the solid state. The unit cell parameters vary slightly depending on the interstitial solvent (*i.e.* 1,2-dichloroethane $(CH_2Cl)_2$ or 1,1,2,2-tetrachloroethane $(CHCl_2)_2$)).

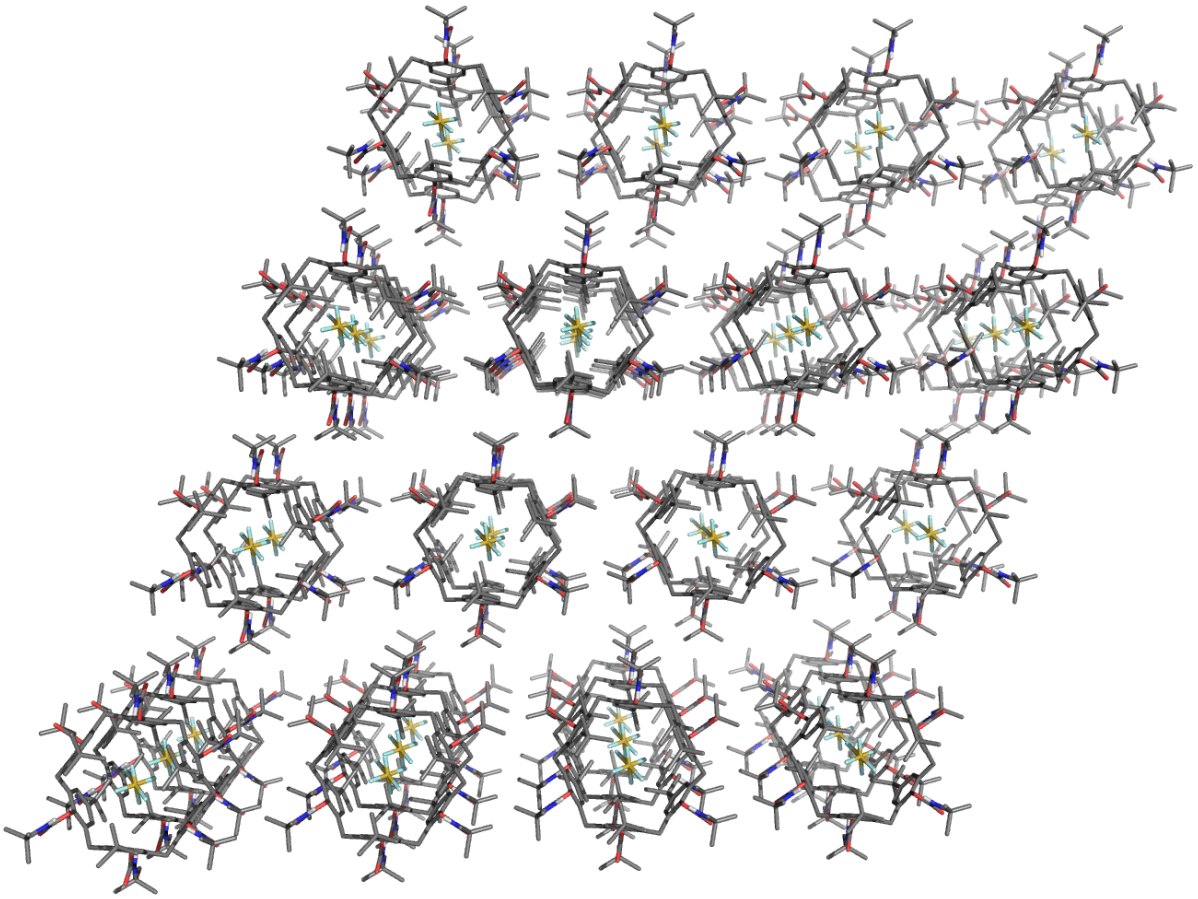

Figure S32. Crystal packing of SF_6@**4** viewed of along the "top" unit cell axis. The Boc and Bac groups cannot be distinguished by XRD due to rotational disorder of the calixarene skeleton and were thus placed arbitrarily. External solvent molecules and non-polar hydrogen atoms were removed for clarity purpose.

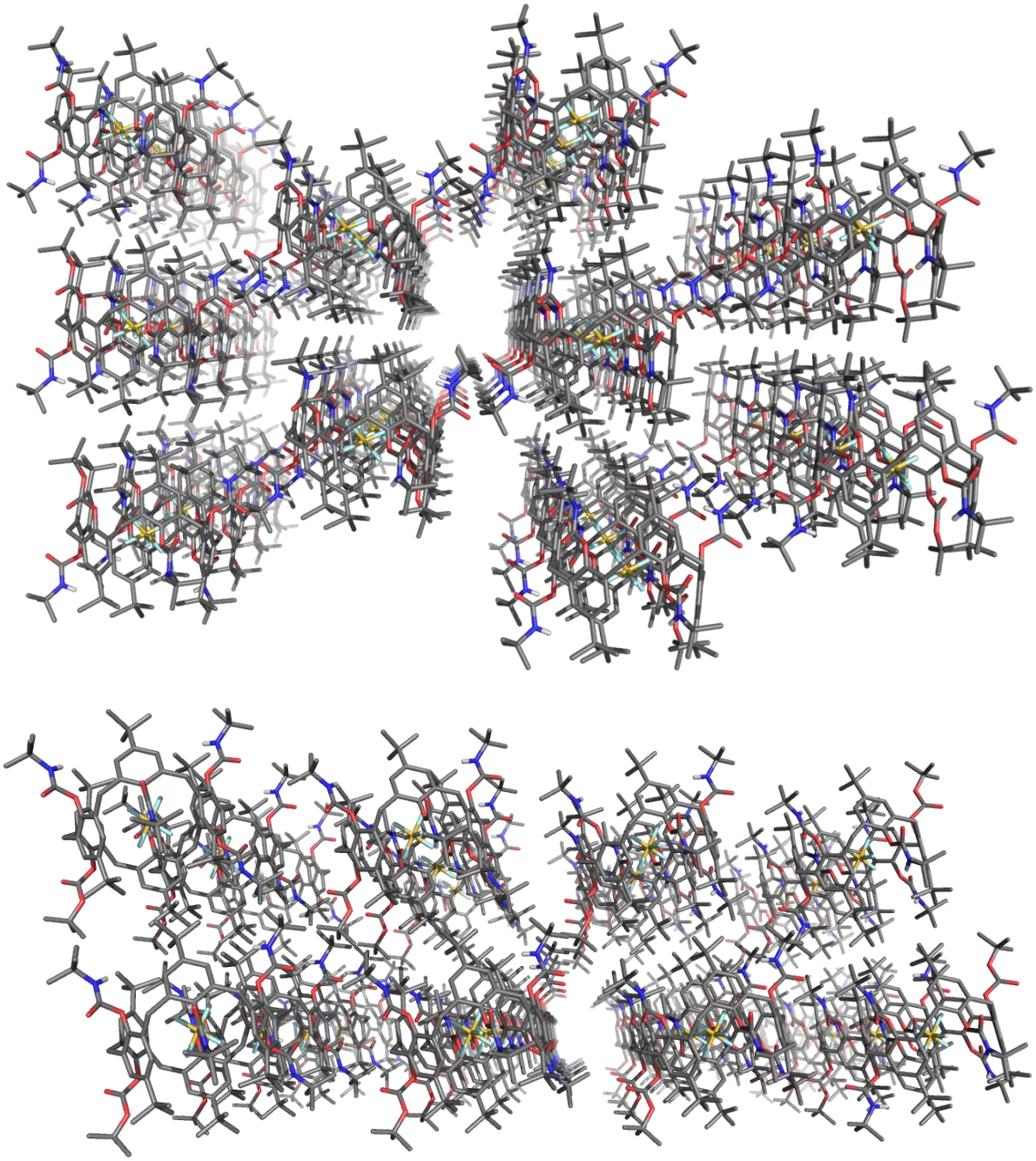

Figure S33. Crystal packing of SF_6@**4** viewed of along the two "side" unit cell axes. The Boc and Bac groups cannot be distinguished by XRD due to rotational disorder of the calixarene skeleton and were thus placed arbitrarily. External solvent molecules and non-polar hydrogen atoms were removed for clarity purpose.